Title

EFFECT OF BAFFLING AND IMPELLER GEOMETRY ON INTERFACIAL AREA IN AGITATED TWO-PHASE LIQUID SYSTEMS

Authors

Rea, H.E.
Vermeulen, T.

Publication Date

1953-04-03

UCRL- 2123

UNCLASSIFIED

UNIVERSITY OF CALIFORNIA — BERKELEY

RADIATION LABORATORY

DISCLAIMER

TECHNICAL INFORMATION DIVISION

Lawrence Radiation Laboratory

Berkeley

Loan to

Assigned to INFORMATION DIVISION

Route to	Noted
M. Smith	✓ NOV 11 1963

Please return this document to the Information Division. Do not send it to the next person on the list.

Please do not remove this page.

UCRL-2123
Unclassified-Chemistry Distribution

UNIVERSITY OF CALIFORNIA

Radiation Laboratory

Contract No. W-7405-eng-48

EFFECT OF BAFFLING AND IMPELLER GEOMETRY ON INTERFACIAL AREA IN AGITATED TWO-PHASE LIQUID SYSTEMS

H. E. Rea, Jr. and T. Vermeulen

April 3, 1953

Berkeley, California

TABLE OF CONTENTS

INDEX TO FIGURES

INDEX TO TABLES

EFFECT OF BAFFLING AND IMPELLER GEOMETRY ON INTERFACIAL AREA IN AGITATED TWO-PHASE LIQUID SYSTEMS

H. E. Rea, Jr. and T. Vermeulen
Department of Chemistry and Chemical Engineering
University of California, Berkeley, California

I. ABSTRACT

This investigation was undertaken to extend previous measurements of the interfacial area formed under baffled conditions of agitation in a cylindrical tank, and to measure the interfacial area formed under unbaffled conditions. Interfacial areas were determined by light transmission measurements through the unstable emulsion formed during agitation.

Impeller geometry was one of the physical variables of the system which was studied. In tests with four-bladed flat paddles at equal speed, the interfacial area was found to increase more than linearly with paddle length, but to be independent of paddle width; it was concluded that the drop diameter is controlled by the highest intensity of turbulence reached at any point in the tank.

The effect of physical properties of the fluids, stirring speed, impeller geometry, and relative proportions of the two phases on interfacial area have also been studied. No generalized correlation for all of the variables was obtained. However, it was found that for each system investigated,

$$A = (\text{constant})\ 6\phi\ e^{-2.0(\phi)^{0.5}}\ NL^{1.5}$$

where A = interfacial area, cm^2/cm^3; ϕ = volume fraction of the dispersed phase, cm^3/cm^3; N = stirring speed, rev/sec; and L =

impeller diameter, cm; the constant having a different value for each system and for each condition of baffling. Mean drop diameters were found to be approximately 1.5 times larger in the case of unbaffled tanks.

Power requirements for the agitation of these systems were also investigated and were found to be identical with those for a homogeneous liquid of equal mean density. For similar impellers, the power required in an unbaffled tank was about one-fourth that in a baffled tank at the same speed. However, both cases showed about equal power for equal interfacial area, for a given impeller geometry. The results indicate high values of interfacial area may be obtained under mixing conditions that will require the minimum power consistent with homogeneous dispersion, in any specific system.

EFFECT OF BAFFLING AND IMPELLER GEOMETRY ON INTERFACIAL AREA IN AGITATED TWO-PHASE LIQUID SYSTEMS

H. E. Rea, Jr. and T. Vermeulen
Department of Chemistry and Chemical Engineering
University of California, Berkeley, California

II. INTRODUCTION

The use of the unit operation of liquid-liquid extraction is widespread as a means of separating components of a solution. However, the factors affecting the contact efficiency of the two liquid phases are only qualitatively understood at the present time. In liquid-liquid systems, agitation is commonly employed to increase the contact between the two phases.

Many investigations (7, 9, 18) have been made to determine the contact efficiency in related agitated systems. Hixson and Tenney (9), who measured the sand-suspending characteristics of a propeller in water and sucrose solutions, suggested the use of the mixing index as a criterion of dispersion. The mixing index as defined by these authors is the average value of the ratios of sand concentration at various points in the apparatus to the concentration that should exist in a completely uniform distribution. The application of the mixing index to liquid-liquid systems is of little usefulness because of the fact that once uniform distribution is attained, the mixing index will fail to show any further increase in the interfacial area upon increased agitation efficiency.

The use of the rate of a heterogeneous reaction as a criterion of agitation efficiency, as proposed by Hixson and Crowell (7), is

not of general utility due to the fact that the rate-determining mechanism may vary widely from one reaction to another.

Miller and Mann (18) have suggested that the power per unit volume be used as a criterion of agitation efficiency. Langlois (11) showed that this criterion is a fair approximation for geometrically similar mixing vessels and impellers, but did not study cases where the geometry is dissimilar.

In considering the factors affecting the rate of mass transfer in agitated two-phase liquid systems, the rate at which mass transfer can occur will depend fundamentally on the interfacial area between the two phases. Because no basis was available until recently for evaluating the interfacial area, very little work has been done with liquid-liquid systems. The criteria of agitation described above are of little use in relating the effect of the operating variables, because it is not known how the rate of mixing two immiscible fluids, or the proportionate suspension of a sand in a liquid (mixing index) is related to the production of interfacial area in an agitated two-phase liquid system.

Measurement of Interfacial Area

Langlois (11) found recently that the interfacial area of an agitated mixture of immiscible liquids could be measured by means of light transmission measurements through the emulsion formed upon agitation of the two liquid phases. He obtained photographs and light transmission measurements simultaneously for various systems of immiscible transparent (i.e., non-absorbing) liquids over a range of stirring speeds from 100 to 400 rpm and for volume fractions of the dispersed phase of 10, 20 and 40 percent. Volume

fraction is defined here as the volume of the dispersed phase divided by the total volume of the two phases under consideration. By measuring and counting the droplets in the photographs, interfacial areas corresponding to light transmission measurements were obtained.

Langlois found that a straightforward relationship existed between the specific surface, expressed as square centimeters of interfacial area per cubic centimeter of volume, and the reciprocal of the fractional light transmission, I_o/I; I_o being the light transmission through the continuous phase alone, and I being the light transmission through the emulsion. This quantity, I_o/I, will be referred to as the extinction ratio in subsequent discussions. In every case, a plot of the extinction ratio versus the specific surface was found to be a straight line with an intercept of unity, corresponding to a functional relationship of the type:

$$\frac{I_o}{I} = \beta A + 1 \qquad (1)$$

This relationship is independent of the volume fraction of the dispersed phase and of the stirring speed over the range studied.

Langlois also found that the slope of Equation (1), β, was different for each system that he investigated, and that a plot of these slopes versus the refractive index ratio, m, for the two media yielded a smooth curve for values of m less than unity, and also for values of m greater than unity, with a discontinuity in slope at m = 1. Here m is defined as the ratio of the refractive index of the dispersed phase to that of the continuous phase, i.e.,

$$m = \frac{n_d}{n_c} \qquad (2)$$

As a result, if the light transmission probe is properly calibrated, it is necessary only to measure the light transmission through the emulsion in order to evaluate the specific area of a homogeneous dispersion of one liquid in another.

Power Requirements

A number of investigations have been carried out to determine the power requirements of fluid systems undergoing agitation (3, 4, 6, 8, 9, 10, 14, 16, 22, 23, 24, 27). These investigations have covered a large range of vessel size and shape, impeller geometry, impeller speed, and fluid properties, so that considerable information now exists which may be used for the prediction of the power requirements for a given agitated system. Most of these data, however, were obtained for the agitation of single-phase liquid systems in baffled and unbaffled tanks, although some of the data (14, 18) were obtained for the agitation of two-phase liquid systems in unbaffled tanks. To date, no study has been made of the power requirements for the agitation of two-phase liquid systems in baffled tanks.

Effect of Physical Variables on Mean Drop Diameter

Although some data are available on liquid-liquid systems, the major portion of the published data on drop diameters in unstable heterogeneous fluid systems have been obtained in connection with the breakup of liquid jets in air (1, 5, 12, 13, 17, 19, 20, 21, 26).

Jets: Haenlein (5) has shown that continuous jets of several different liquids issuing from a circular nozzle into

gaseous surroundings are unstable with respect to the surface forces acting upon it. Initial disturbances, such as vibration of the injector and imperfect roundness of the orifice, cause certain characteristic deformations which are a function of velocity for any particular liquid.

Merrington and Richardson (17) found that the mean drop diameter was proportional to the kinematic viscosity of the liquid to the 0.2 power, inversely proportional to the linear velocity of the liquid, and independent of the surface tension over the range of 25 to 73 dynes/cm. They also obtained data on jets of liquids into other liquids, which did not agree well with those obtained for liquid jets into air. No explanation for this difference was offered by the authors.

Lewis and co-workers (13) correlated a good deal of existing data on drop diameters obtained from venturi-type atomizers, using an empirical equation developed by Nukiyama and Tanasawa (19-21):

$$d = \frac{585}{u}\sqrt{\frac{\sigma}{\rho_d}} + 597\left(\frac{\mu_d}{\sqrt{\rho_d \sigma}}\right)^{0.5}\left(1000\,\frac{Q_1}{Q_2}\right)^{1.5} \qquad (3)$$

where d = mean drop diameter, that diameter having the same surface to volume ratio as the total sum of drops, microns

u = relative velocity of liquid and gas, meters/sec.

Q_1/Q_2 = ratio of volume flow rate of liquid to volume flow rate of gas

ρ_d = liquid density, gm/cc.

μ_d = liquid viscosity, poises

σ = surface tension, dynes/cm.

This equation was reported to correlate adequately the results of a number of measurements, including those data obtained with ordinary hydraulic jets, once a number corresponding to the ratio Q_1/Q_2 has been determined for a given nozzle.

Laminar Flow Fields: From a study of the breakup of a liquid droplet in laminar flow fields, Taylor (26) developed a dimensionless parameter, F (see Nomenclature). He found that the droplet burst at a characteristic value of this parameter, F_c. He also found that F_c was a function only of the ratio of continuous phase viscosity to dispersed phase viscosity, to about the 0.15 power. In another apparatus, for values of this viscosity ratio greater than unity, F_c was approximately proportional to the 5.5 power of this ratio.

Taylor thus concluded that, when bursting of a droplet is the result of simple shearing action in a laminar flow field, the dependence of drop diameter on the viscosity of the two phases will vary considerably with the type of shearing action. His conclusion serves to emphasize the difficulty of predicting the effects of fluid properties on drop diameters when the flow field is not a laminar one but a complex turbulent one.

Agitated Systems: Data on drop sizes in agitated two-phase liquid systems are reported by Clay (2), who studied emulsion formation in turbulent flow for liquids covering a range of densities from 0.78 to 1.19 gm/cc, of viscosity from 0.6 to 37 centipoises, and of interfacial tension from 1 to 47 dynes/cm. Drop sizes, determined by high speed photography, were obtained from a "technical apparatus" and a "model apparatus".

In the technical apparatus, which consisted of a circuit of four-inch i.d. pipe in series with a pump, Clay assumed that the majority of bursting of droplets resulted from turbulence in the pipe, particularly at the bends in the pipe, and that the contribution of the pump to emulsion formation was negligible. This assumption seems somewhat doubtful.

In the model apparatus, which contained the emulsion in the annular space between two cylinders, the agitation of the two liquids occurred as a result of the rotation of the inner cylinder.

In interpreting his data, Clay proposed two possible mechanisms of the bursting of droplets. In the first mechanism, Clay postulated that, if bursting were accomplished by shearing action resulting from velocity gradients within the liquid, the diameter of the largest drop which would be stable in the model apparatus would be given by the expression,

$$\frac{2\sigma}{d} = k \cdot \frac{\rho_c (NR_1)^2}{\sqrt{Re_m}} \qquad (4)$$

Here Clay assumed that the disruptive forces necessary to burst the droplet would be proportional to $2\sigma/d$. If this mechanism were dominant, then $2\sigma/d$ $\rho_c(NR_1)^2$ would be proportional to the inverse square root of the Reynolds number for the model apparatus, Re_m.

In the second mechanism, Clay assumed that the droplet would burst whenever the pressure at its surface fell to a value below the mean, and that the diameter for the largest stable drop for this mechanism would be given by the expression,

$$\frac{2\sigma}{d} = k \rho_c (NR_1)^2 \qquad (5)$$

and in this case $2\sigma/d\ \rho_c(NR_1)^2$ would be independent of the Reynolds number, Re_m.

This quantity, $2\sigma/d\ \rho_c(NR_1)^2$, was calculated by Clay for all the model apparatus experiments and plotted against the Reynolds number. The data scattered very badly. Clay concluded that since this quantity appeared to be independent of the Reynolds number, the second mechanism was almost solely responsible for the bursting of the droplets. Since Equations (4) and (5) were not derived by any rigorous mathematical development, and that there exists the possibility of other mechanisms of bursting, the most that can be concluded is that the latter mechanism was somewhat more important than the former.

Langlois (11) obtained drop diameters for two-phase liquid systems by the agitation of these systems in a baffled cylindrical tank. He used liquids covering a range of densities of 0.69 to 1.60 gm/cc, density-differences from 0.03 to 0.60 gm/cc, viscosities from 0.38 to 184 centipoises, and interfacial tensions from 3.6 to 55.1 dynes/cm. For any given liquid-liquid system, he found that at a given speed of agitation the mean drop diameter, that diameter having the same surface to volume ratio as the total sum of drops, was an exponential function of the volume fraction. The slopes of log d versus volume fraction plots were found to vary with the stirring speed and the fluid properties of the liquids used. By plotting the values of these slopes against the Weber number, he obtained the following equation relating the mean drop diameter to volume fraction:

$$\text{Log } d = 0.46\,\phi\,We^{0.19} + \log d_o \qquad (6)$$

where d = mean drop diameter, cm

ϕ = volume fraction of dispersed phase, cc/cc

We = Weber number = $N^2L^3\,\rho/\sigma$.

The data used to determine the exponent of the Weber number in Equation (6) scattered badly. This he attributed to the fact that the difference in the mean drop diameters existing at two different volume fractions was not a great deal larger than the experimental error in reproducing the emulsions.

In attempting to find a general correlation for the effect of all variables, he found it more convenient to use a fictitious drop diameter, d_o, the mean drop diameter extrapolated to zero volume fraction of dispersed phase. He found the following dimensionless expression to fit the data satisfactorily:

$$\left(\frac{d_o}{L}\right)^{3/4}\left(\frac{NL^{3/2}\sqrt{\bar{\rho}}}{\sqrt{\sigma}}\right) = 0.21 \qquad (7)$$

By combining Equations (6) and (7) with the relationship between the square centimeters of interfacial area per unit volume and drop diameter, i.e. $A = 6\phi/d_o$, he obtained as a final correlation of his data the following expression:

$$\frac{A\sigma^{0.67}}{N^{1.33}\,\bar{\rho}^{0.67}L} = 48\phi\,\exp\left[-0.46\phi\left(\frac{N^2L^3\bar{\rho}}{\sigma}\right)^{0.2}\right] \qquad (8)$$

This correlation is highly dependent upon the values of d_o obtained by Equation (6). The exponent of the Weber number in Equation (6) was evaluated with data over a 16-fold range in the Weber number, whereas the data used to calculate the values of d_o from Equation

(6) had a 225-fold range in the Weber number. In view of the scatter of the plot which was used in determining the exponent of the Weber number in Equation (6), it is quite probable that Equation (8) is not applicable over the 225-fold range of Weber number.

Purpose of Present Investigation

The primary objective of this investigation was to study the effect of the physical variables in agitated two-phase liquid systems on the formation of interfacial area. Impeller geometry especially was studied more fully than in any previous investigation. It was desired to extend previous measurements of interfacial area formed under baffled conditions, and to measure the interfacial area formed under unbaffled conditions. Earlier studies of the effect of volume fraction upon interfacial area were indecisive, and this factor was also given attention.

The secondary objective was to determine the power requirements for the agitation of these systems under baffled and unbaffled conditions. It was desired to measure the effect, if any, of the production of interfacial area and the relative volume proportions of the two liquid phases on power consumption. It was expected, but not found, that the extent of interfacial area might have a small effect on power consumption, which might have theoretical significance. For single-phase liquid systems (23, 24) density is the only physical property of the fluid that affects power requirements in the turbulent region of flow, hence fluids covering a wide range of densities were employed.

The variables which were considered to be pertinent in this study were: 1. The physical properties of the two liquid phases, e.g. viscosity, density, and interfacial tension. 2. The volume fraction of dispersed phase. 3. The stirring speed. 4. Factors characterizing the geometry of the impeller. 5. The effect of scale-up conditions.

III. EXPERIMENTAL PROGRAM

Systems Investigated and Materials

Interfacial areas resulting from the dispersion of iso-octane (2, 2, 4-trimethyl pentane), carbon tetrachloride, carbon disulfide, n-butanol, and methyl isobutyl ketone in water and the dispersions of water in these liquids were determined in the small baffled tank. Interfacial areas were also obtained in the large baffled tank for the system methyl isobutyl ketone-water. Interfacial areas were measured in the small unbaffled tank for the systems: carbon tetrachloride-water, carbon disulfide-water, and methyl isobutyl ketone-water. All measurements were made at $20 \pm 0.5^{\circ}$ C.

The physical properties of the equilibrated phases for these systems were determined at 20° C. and are listed in Table 2. Prior to agitation and subsequent measurement of interfacial area, the two liquid phases were saturated with respect to each other.

For the purpose of calibrating the light transmission probe, interfacial areas were determined for the systems which Langlois (11) measured photographically (see Table 3). These runs also served to determine the reproducibility of the equipment and measurements, gave additional information on the volume fraction dependence and

on the phase shift, provided data on power consumption.

Agitation Apparatus

Mixing Equipment: Two cylindrical stainless steel tanks, one approximately ten inches in diameter and height and the other twenty inches in diameter and height, were used in this investigation. Four vertical baffles spaced at 90° intervals around the tank were mounted against the tank wall and at right angles to it. Mack and Kroll (15) have shown this number of baffles to represent a condition of "standard baffling" (so termed by J. H. Rushton (25)). A cooling coil was soldered to the outside of each of the tanks, through which cooling water could be circulated for temperature control.

The small tank was mounted to the frame, which was constructed of five-inch channel iron, by means of an integral-suspension ball-bearing unit welded to the tank cover. A collar, which was welded to the upper side of the frame and center-lined with respect to the tank cover assembly, contained a spindle assembly with two sets of ball bearings to which the impeller shaft was connected. The two sets of ball bearings were located as far apart as possible so as to minimize any whip the impeller might have. The final assembly of these units permitted the free rotation of the tank cover assembly and the impeller shaft, each independent of the other, thereby enabling the determination of the power required for mixing by torque measurements.

The tank itself was fastened to the tank cover by the use of L-shaped wing nuts. A gasket groove, into which a cork gasket

was cemented, was provided to ensure liquid-tight contact between the tank and the cover. A mercury seal was used to make the impeller shaft seal liquid- and air-tight.

The small tank cover contained a mounting for a light transmission probe, the construction of which will be described in detail in the following section; two holes tapped for 1/4 inch pipe for feed lines to the tank; and a combination thermometer well and vent hole tapped for 1/8 inch pipe thread. These were spaced at ninety degree intervals around the tank cover and located so that they would be forty-five degrees out of phase with the baffles in the tank. A 1/2 inch pipe outlet was located in the center of the tank bottom.

The bottom of the large tank was mounted on the bottom of the channel iron frame by means of a ball thrust bearing assembly. The tank cover for the large tank was mounted to the frame through a self-aligning ball bearing unit, above which was another spindle assembly similar to that of the small tank assembly. This final assembly also allowed independent rotation of the tank and impeller shaft.

Whereas in the small tank assembly, the tank was removed by lowering the tank from the tank cover, the large tank assembly was designed so that the tank cover and shaft assembly could be lifted from the tank. This was done by attaching the channel iron across the top of the frame over the large tank to a supporting bracket post which could slide up and down in its mounting on the lower portion of the frame. To remove the large

tank cover, the upper channel iron was unbolted, the tank cover unbolted from the tank, and the tank cover, channel iron, spindle assembly, impeller shaft, and impeller were lifted manually from the tank as a unit. When the bracket post was at its uppermost traverse, high enough to allow the tank cover assembly including the impeller shaft and impeller to swing out clear of the tank for the purpose of changing impellers in the large tank, a spring would pull a post stop underneath the bracket post, thereby holding the assembly in position at its maximum height.

The large tank cover also contained a mounting for a light transmission probe, two holes tapped for 1/2 inch n.p.s. for feed lines into the tank, and a combination thermometer well and vent hole tapped for 1/4 inch n.p.s. These were also spaced at ninety degree intervals around the tank cover and forty-five degrees out of phase with the baffles in the tank. A 1/2 inch n.p.s. product line was located in the center of the tank bottom, passing directly through the thrust bearing seat. The large tank was also equipped with a mercury seal to make the impeller shaft seal liquid- and air-tight. A cork gasket was employed to make the contact between the tank and tank cover liquid tight. On both tanks, provision was made to protect the ball bearing units from any mercury that might be blown out through the ball bearing units. No difficulty was experienced, however, in the blowing of the mercury seal.

A slight pitch was built into the bottom of the large tank to ensure complete drainage upon emptying the tank when changing

from system to system. The small discrepancy in the geometric similarity between the two tanks is due to the fact that the small tank was a prefabricated tank, whereas the large tank was constructed for this investigation.

A tang was provided at the bottom of each impeller shaft to lock the impeller into position horizontally. A threaded extension of the shaft beyond the tang permitted the use of lock nuts to hold the impeller in place vertically.

Three sizes of impellers were used in the small-tank investigations: A2, 5.00 inches in diameter and 0.94 inch in width; A3, 7.50 inches in diameter and 0.94 inch in width; and A4, 6.67 inches in diameter and 1.65 inches in width. The latter impeller was used in the calibration of the light transmission probe.

Four sizes of impellers were used in the large-tank investigations: B1, 5.00 inches in diameter and 2.00 inches in width; B2, 10.00 inches in diameter and 2.00 inches in width; B3, 15.00 inches in diameter and 2.00 inches in width; and B4, 13.00 inches in diameter and 3.72 inches in width.

The impellers in both tanks were driven through a V-belt drive by a 3/4 horsepower, 3-phase, 60-cycle, 220-volt, 216 rpm right-angle ring-mounted gear motor supplied by Electra Motors, Inc., of Anaheim, California. V-step cone pulleys were mounted on each of the impeller shafts and on the motor shaft. The four steps in the pulleys permitted the operation of the impellers at 94, 154, 247, and 394 rpm.

Figure 1 is an assembly drawing of the tanks showing in detail their construction, along with the assembly of the ball bearing units, the cups for the mercury seal, and other features of the design. Figure 2 is a photograph of the final assembly. Complete dimensions of the tanks, baffles, and impellers are given in Table 1.

Light Transmission Probes: The light transmission probes consisted of two parts. The lower section contained a light source which was a small penlight lamp, and the upper section contained a photoelectric cell. Countersunk into the housing directly in front of these two units were windows made of Corning Filter Glass, number 3962 (also labeled CS 1-57). The glass-to-metal seal was made with Araldite cement, which is a thermosetting polymer. These two units were mounted in a unit assembly of stainless steel so that there was a gap of 1.0 centimeter between the outer surfaces of the two glass windows, i.e., those surfaces in contact with the liquid-liquid emulsion. Light transmissions across this gap were measured by the photoelectric cell. The penlight lamp had a built-in lens which resulted in a beam of nearly parallel light so that no collimating system was necessary.

The light transmission probe for the large tank was an exact duplicate of that for the small tank, with the exception of its length. The depth to which the center-line between the glass windows was immersed was geometrically proportional to the corresponding depth in the small tank. In addition, the probe mounting for the large tank was designed so that the light transmission probe could have a vertical traverse. This permitted the observation of any

variations which might exist in the light transmission readings due to the depth of the probe, i.e., variations due to the absence of uniform mixing conditions could be studied.

The light transmission probes in both tanks were inserted and mounted into place so that the gap between the glass windows would face the center of the tank. A half-diameter of the probes protruded inside (i.e., to the center) the circle diameter formed by the baffle edges away from the tank wall. When the tanks were baffled, the positioning of the probes in such a manner would not affect the mixing characteristics of the various impellers employed and would ensure light transmissions through emulsions representative of the tank contents. The probes were held in position on their mounting by means of Allen-head set screws, and a Tygon gasket made the junction liquid-and air-tight. The distance between the under side of the tank cover and the center-line between the glass surfaces of the small-tank probe was 1-3/8 inches. The solid portion of the probe on the back side (i.e. next to the tank wall) was bored for wire leads to the penlight lamp. Two holes were drilled on either side of this bore at a height midway between the glass windows, to ensure rapid circulation of the emulsion through the 1.0 centimeter gap between the windows.

Figure 3 is an assembly drawing of the large-tank light transmission probe, and Figure 4 is a photograph of the small-tank light transmission probe. Inspection of Figure 2 will show the large-tank light transmission probe mounted in position in the tank cover.

The small-tank light transmission probe used in this investigation was calibrated by obtaining light transmission measurements during the agitation of the same liquid-liquid systems in an apparatus identical to that used by Langlois in determining the interfacial area photographically. The results of this calibration are given in Table 3 where the specific area and the corresponding light ratios, I_o/I, are listed for the various liquid-liquid systems. Figures 7-11 are plots of the light ratio against the specific area, and Figure 12 is a plot of the slopes, β, of Figures 8-11 against the refractive index ratio, m. Interfacial areas for additional liquid-liquid systems were determined by measuring the light transmissions through the emulsions obtained, reading a value of β for the particular system being studied from Figure 12, and calculating the specific area.

The large-tank light transmission probe used in this investigation was calibrated against the small-tank light transmission probe. The following equation was used to correct the reading obtained using the large-tank light transmission probe.

$$(\beta)_{\text{large tank}} = 0.9533\,(\beta)_{\text{small tank}} \qquad (9)$$

Figure 13 is a cross-plot of β values obtained with the probe in this investigation with those obtained by Langlois. As can be seen, there exists a considerable difference in the calibration of the probe used in his investigation and that of the present work. The internal construction of the probes used in this work was designed to be identical to Langlois' probe. Thus, the penlight

lamp was mounted at an identical distance from its glass window, and the cathode of the photoelectric cell was an identical distance from its glass window. Since it was thought that the liquid flow pattern around the probe might account for the differences in the calibration, the small-tank light-transmission probe was rotated in its mounting and light transmission readings obtained, and it was found that rotation of the probe had no effect upon the light transmissions. It was observed that the geometries of the photoelectric cells are not identical; to determine whether this could explain the difference in calibration, the photoelectric cell was also rotated and light transmission readings obtained; in addition, light transmission readings were obtained using several different photoelectric cells. A slight change in the light transmissions (possibly 0.5 percent) resulted from the rotation and replacement of the photoelectric cell, which was negligible in comparison to the difference in calibrations.

It was decided that the solid surface where the two circulation holes were drilled served as a reflection surface and thereby increased the value of the light transmissions obtained with the probe used in this investigation, particularly for the liquid-liquid systems with high and low values of the refractive index ratio, m. This surface was not present in the probe used by Langlois. In order to obtain standard readings, it is recommended that the outer surfaces of future probes be permanently blackened to eliminate reflection.

Power Measurements

The two mixing tanks were mounted with ball bearing units, previously described, which allowed the rotation of the tanks with a negligible amount of friction. The torque necessary to prevent the tanks from turning in the direction of rotation of the impeller was recorded and used to calculate the power required for agitation. The following expression for brake-horsepower was used to calculate the power required:

$$P = 2\pi R N T \qquad (10)$$

where P = agitator shaft power, ft-lbs/min

N = agitator speed, rpm

R = dynamometer torque arm, ft

T = dynamometer balancing force, lbs.

The dynamometer balancing force was measured by a Toledo Scale, Model 4021 BA, (Number 874285) which had a capacity of 30 pounds and a two-pound dial scale reading graduated to 0.01 pound. This was connected to a stud on top of the tank by a cord and a nearly frictionless pulley mounted on the supporting frame. Readings taken with the scale were found to be reproducible to within 0.03-0.04 pound.

Light Transmission Measurements

The current to burn the penlight lamp was drawn from a six volt lead storage battery. A Leeds and Northrup students' potentiometer (Number 635112), in conjunction with a Rubicon d.c. galvanometer (No. 3829), (with a sensitivity of .036 micro-amperes per millimeter) was used to measure the potential drop

across the filament. A variable resistance was provided in the circuit by means of which a given e.m.f. could be applied to the filament and held constant, thus assuring a constant light intensity during any one experiment. The lamp, which was designed to be burned at about 2 volts, was burned at only about 1 volt so that there would be no tendency for the lamp filament to deteriorate over a period of time. The circuit for the light source is shown in Figure 5.

The photoelectric cell used in this work was a commercial cell, the RCA 1P41, which consists simply of a photosensitive cathode plate and an anode. A potential of 90 volts was placed across the cell in order that all electrons emitted by the cathode would be caught by the anode. Current flowing through the cell was measured by a sensitive galvanometer. A sketch of the photoelectric cell circuit is shown in Figure 6.

The galvanometer used in this circuit was a Leeds and Northrup Type 2430 D direct-current galvanometer, (Number 1014406) with a sensitivity of 0.00042 microamperes per millimeter. The photoelectric cell would not remain stable when subjected to continuous currents much in excess of 2 microamperes; this fixed the upper limit of the light intensity at 100 percent transmission, that is, when no emulsion was present. The galvanometer sensitivity was selected to give 2 percent accuracy on light transmissions as low as 1 percent. A shunt was placed in the circuit so that, by suitable adjustment of the variable resistance, a large deflection could be obtained even at low values

of the light transmission, with consequent increased precision in the readings obtained. The variable resistances were adjusted in such a way that the total resistance was equal to 24,000 ohms, the critical damping resistance of the galvanometer. The total current flowing from the photoelectric cell was calculated from the indicated galvanometer current, using the known values of the two variable resistances and the galvanometer resistance. Because of the very small currents being measured, considerable trouble was experienced with stray currents. This difficulty was surmounted by mounting the whole photoelectric cell circuit on a metal plate and grounding the circuit to the plate at the point indicated on the diagram.

The current flowing through the photoelectric cell is directly proportional to the intensity of the light falling upon it. By taking a ratio of the current under two different situations, the constant of proportionality cancels and the ratio of the photoelectric cell currents is equal to the ratio of the light intensities. In this investigation, an initial value of the current, I_o, corresponding to the initial light intensity was obtained before the stirring was started, that is, with only the continuous phase between the light source and the photoelectric cell. Values of the current, I, were subsequently obtained while stirring with the emulsion between the light source and the photoelectric cell, and the ratio of these two quantities, I/I_o, is equal to the fractional light transmission.

The colored filter glasses used as the window plates in front of the photoelectric cell and the light source were used to filter

out the infrared radiation of the light source, in order to narrow the wavelength range and thus sharpen the refractive index ratio. From a consideration of the characteristics of the light source and the filter glass and the photoelectric cell sensitivity, it was concluded that the bulk of the current resulted from light in the range from 7000-8000 Å. The refractive indices of the liquids were used in the correlation of the light transmission data, and, strictly, the refractive index at 7500 Å should have been used. However, the refractive index appeared in all of the calculations as a ratio, and the change in refractive index with wave length for the various liquids used is sufficiently similar (for five liquids on which data were available) so that there is a negligible difference between the ratio of the indices at 5893 Å (the sodium D line) and the ratio of the indices at 7500 Å. Consequently, the more easily obtained values of the refractive index at the sodium D line were used.

Araldite cement was used for cementing the filter glass windows to the probe housing. The Araldite was melted onto the glass and metal surfaces by means of a gas flame and then cured by baking at 200° C. for 1 hour and at 150° C. for two hours. This cement was found to be satisfactory for all of the liquids handled in this investigation if a good bonding to the metal is obtained. As a safety precaution, in order to prevent any damage to the bonding, the probe unit was removed from the apparatus at the end of a series of runs and dried out.

Operating Procedure

In making each experimental run for the measurement of

interfacial areas, the following procedure was followed: the tank was cleaned and rinsed thoroughly with the polar solvent, usually water. The light transmission probe was placed in the tank, and the tank charged with the continuous phase. The initial light intensity, I_o, was then observed. This was done before adding the dispersed phase because, if the latter were the upper layer, the interface between the two phases for the small volume fractions, which were used to start the series of runs, usually passed through a plane which lay between the light source and the photoelectric cell. Thus, this would give an incorrect value of the initial light intensity, I_o. An amount of the continuous phase slightly exceeding that of the desired volume fraction of the dispersed phase was then drained from the tank; the desired volume fraction of dispersed phase added to the tank, and continuous phase liquid added to bring the liquid level in the tank to the top. This procedure eliminated the formation of air bubbles from trapped air in the tank during mixing. Cooling water was circulated to bring the temperature of the tank contents to 20° C and agitation started. It was found that by varying the flow rate of the cooling water through the cooling coils, it was possible to control the temperature easily within $\pm 0.5^{\circ}$ C.

Light transmissions were observed and recorded every thirty seconds from the time agitation was started. When the light transmission had ceased to drop and held constant over a period of time, usually 15 to 30 minutes, the system was considered to be in steady state. The time required to reach steady state varied from system to system and from speed to speed and ranged from

two or three minutes to ten or fifteen. In some cases, the rate of approach to steady state was too fast to be observed.

The indicated light intensity was not steady, but experienced short-term fluctuations. These apparently resulted from small local inhomogeneities in the emulsion. The magnitude of these fluctuations was rather large at the lowest stirring speed; the fluctuations frequently amounting to several percent. At the higher speeds, the fluctuations were much smaller. This does not necessarily mean that the emulsions were more homogeneous at the higher speeds, but might merely indicate that the galvanometer did not have time to react to them. In all cases, an average value was estimated for the current, and this was used in the calculations of the extinction ratio. The variations of area or mean diameter values from smoothed curves indicates a precision of $\pm$ 5%, which is superimposed upon an additional uncertainty of $\pm$ 10% due to the probe calibration.

After the steady-state light transmission readings had been obtained, power readings were taken. The power readings experience very rapid fluctuations, particularly at the higher speeds where there was a higher degree of turbulent motion of the fluids. The average fluctuations in the power readings were approximately five percent at the highest speed. At the low speeds the fluctuations were negligible. A series of twenty readings were taken at thirty second intervals, and the average of these values taken as the power reading. In all cases, the rate of approach to steady state for the power readings was too fast to observe.

Although a direct comparison of fluctuations in baffled and unbaffled tanks was not made, much less fluctuation was observed in the unbaffled systems.

By observing the continuity of the I_o/I readings, it was possible to determine which phase was dispersed. With the exception of the butanol-water system, the phase shift occurred at or near 50 percent volume fraction point. For butanol-water, this shift occurred at 60 percent butanol. This agrees with observations made by Long (14).

After a value of light intensity and power had been obtained at one speed for a given volume fraction of dispersed phase, the stirring speed was increased, and a new set of readings for these quantities was obtained. After light transmissions and power readings were determined for the four stirring speeds used, the volume fraction of dispersed phase was changed, and the light transmissions and power readings were determined for this new volume fraction.

When a complete set of light transmission and power data had been obtained for a given system for all of the desired speeds and volume fractions of dispersed phase, the tank contents were drained, the tank removed, and the impeller changed. A complete set of light transmission and power data were then determined for the new impeller.

IV. POWER REQUIREMENTS

Power data obtained on single-phase systems have been correlated using two dimensionless groups: a power number and a Reynolds number.

$$\text{Power Number} = P_o = Pg/\rho N^3 \cdot 1/L^5$$

$$\text{Reynolds Number} = Re = NL^2\rho/\mu$$

where P = power

g = gravitational constant

N = stirring speed

L = impeller diameter

ρ = liquid density

μ = liquid viscosity,

all in consistent units. The power data obtained in this investigation are given in Tables 4 and 5-17 in Appendix II.

Results and Discussion

Single-Phase Power Data: Single-phase power data were obtained under baffled conditions for all impellers used in this study, for both tanks using water, and for all impellers in the ten-inch tank using carbon tetrachloride. For unbaffled conditions, power data were obtained for all impellers in the ten-inch tank using water, carbon disulfide, and methyl isobutyl ketone and for impeller number A4 for carbon tetrachloride. The power numbers and the Reynolds numbers calculated from these data are listed in Table 4.

It was found that the power number was a constant; the value of this constant varying with the geometry of the impeller

used. By multiplying the power number by the diameter-to-width ratio of the impeller, i.e., L/W, another dimensionless number was obtained, P_w, which had a constant value independent of impeller geometry. Values of P_w for both baffled and unbaffled agitation are given in Table 4.

The purpose of obtaining the single-phase power data was twofold. First, it was desired to determine whether or not any discrepancy existed between the power measurements obtained in this study and those obtained by previous investigators. No discrepancy was found to exist. Secondly, it was desired to establish that the range of Reynolds numbers to be encountered in this investigation would be in the turbulent region of flow. Inspection of Figures 14 and 15 shows that P_o and P_w are independent of the Reynolds number and that such is the case. The plots of Figure 15 can be represented by the equations:

for baffled tank: $$Pg = 19\rho N^3 L^4 W \qquad (11)$$

for unbaffled tank: $$Pg = 6\rho N^3 L^4 W \qquad (12)$$

Two-Phase Power Data: Two-phase power data were obtained under baffled conditions for the dispersions of the systems of iso-octane-water and carbon tetrachloride-water for one impeller geometry, A4, and for the dispersions of the systems n-butanol-water, carbon disulfide-water, and methyl isobutyl ketone-water for all impeller geometries in the ten-inch tank. Power data for the twenty-inch tank were obtained from the dispersions of the system methyl isobutyl ketone-water using all impeller geometries under baffled conditions. Power data were

also obtained for unbaffled conditions for the dispersions of the systems of carbon disulfide-water and methyl isobutyl ketone-water for all impeller geometries in the ten-inch tank, and for the system carbon tetrachloride-water for impeller number A4.

It was found that the use of a volume-fraction-mean density would give values of the number, P_w, corresponding to those obtained from the single-phase power data. Values of P_w are given in Tables 5-17. These data can be represented by the equations:

for baffled tanks: $$Pg = 19\, N^3 L^4 W \left[\rho_c + \phi\,(\rho_d - \rho_c)\right] \quad (13)$$

for unbaffled tanks: $$Pg = 6\, N^3 L^4 W \left[\rho_c + \phi\,(\rho_d - \rho_c)\right] \quad (14)$$

V. EFFECT OF PHYSICAL VARIABLES ON MEAN DROP DIAMETER

Various pairs of liquids listed in Table 2 were agitated together under baffled and unbaffled conditions, and the light transmissions measured. The specific area was calculated using Equation (1). The mean drop diameter was then calculated from the specific area; the mean drop diameter being the diameter of a drop having the same ratio of surface to volume as the sum total of the droplets in the emulsion. The mean drop diameter so defined may be calculated by using the following relation:

$$d = 6\phi/A \quad (15)$$

where d = mean drop diameter, cm

ϕ = volume fraction of dispersed phase, cc/cc

A = specific area, cm^2/cm^3

The effect of the volume fraction of dispersed phase on the mean drop diameter was investigated over the range from 10 to 40 percent and in some cases as high as 60 percent. The effect of stirring speed on the mean drop diameter was studied at speeds of 94, 154, 247, and 394 rpm. A large number of drop diameter data were obtained as a function of the impeller geometry by varying the diameter, and the diameter-to-width ratio, of the impeller. The resulting mean drop diameters are given in Tables 5-17.

Results and Discussion

Effect of Stirring Speed: As would be expected, the mean drop diameter decreased as the stirring speed was increased. The nature of the dependence may be seen in Figure 18 which is a log-log plot of mean drop diameter versus the stirring speed for some typical runs. For the high interfacial tension liquids, this plot is not a straight line but has a slight curvature, so that the relationship between d and N cannot be expressed rigorously by an equation of the form:

$$d = cN^a \tag{16}$$

where c and a are constants. However, for the low interfacial tension liquids, it will be seen that this plot does give a straight line over the range of stirring speeds studied. For both low and high interfacial tension liquids, the best fit of the data for both the baffled and unbaffled conditions of agitation indicates a simple relationship of the form:

$$d = c/N \tag{17}$$

Discrepancies in mean drop diameters observed in this study and that of Langlois at low stirring speeds may indicate incomplete mixing. Data in this region were therefore discounted in attempts to find a general correlation.

The relative rate of increase of interfacial area and power input as the stirring speed is increased may be obtained by combining Equations (15) and (17) to give an equation relating the interfacial area to stirring speed. The power consumption in baffled and unbaffled systems, as given by Equations (13) and (14), is proportional to the third power of the impeller speed. Combination of these equations results in an expression relating power consumption to interfacial area, for the condition where all variables except stirring speed are held constant.

$$A = k P^{0.33} \qquad (18)$$

As the stirring speed is increased, therefore, the power consumption increases much more rapidly than does the interfacial area.

Effect of Volume Fraction of Dispersed Phase: The mean drop diameter was also found to depend on the volume fraction of dispersed phase, becoming smaller as the volume fraction decreased. A dependence of drop diameter on this factor is not unexpected. The processes of coalescence and bursting are both occurring in the mixing apparatus, and in the steady state, the rates of these two processes must be exactly equal so that the total interfacial area remains constant. The frequency of bursting will increase as the degree of turbulence increases and as the drop size increases. The

frequency of coalescence will depend upon the frequency and number of droplets colliding with one another. If it is assumed that the number of coalescences is proportional to the number of collisions between droplets, and if, in analogy to the kinetic theory of gases, it is assumed that the number of collisions is proportional to the square of the number of droplets, the number of coalescences would be proportional to the square of the volume fraction of dispersed phase. As the volume fraction of the dispersed phase is increased, therefore, the rate of coalescence would increase as the square of the volume fraction, whereas the rate of bursting would increase as the first power of the volume fraction. This would result in an unsteady state during which the mean drop size would increase until the rate of bursting had again become equal to the rate of coalescence.

The effect of volume fraction of dispersed phase on the mean drop diameter was determined with five pairs of fluids and in some cases for all geometries in both the small and large tanks for baffled and unbaffled conditions of agitation. The magnitude of the variation in mean drop diameter with volume fraction may be seen in Figure 18 where, for a typical case, the mean drop diameter is plotted as a function of stirring speed with volume fraction of the dispersed phase as a parameter. With all other variables held constant, the mean drop diameter was found to be an exponential function of the square root of the volume fraction, i.e.,

$$\log d = b(\phi)^{0.5} + \log d_o \quad (19)$$

This is shown by Figure 19 where for a typical case log d is plotted against the square root of volume fraction for a number of stirring speeds. The slope of Equation (19), b, was found to be independent of stirring speed and of fluid properties of the systems over the ranges investigated. Inspection of Table 18 shows the average value of the slope, b, for all systems studied to be 2.0. The intercept drop diameter, d_o, of Equation (19) may be tentatively identified with the mean drop diameter at infinite dilution. In this state, no coalescence would occur, and hence, after the initial dispersion, no bursting would occur. Thus, the drops would be stable in the turbulent field of flow. The intercept drop diameter, d_o, should be proportional to, but not identical with, the maximum diameter of a drop capable of existing in the turbulent flow field; drops somewhat smaller than this maximum can be formed during dispersion, and would continue to exist in the absence of coalescence.

Effect of Impeller Geometry: At constant speed, the mean drop diameter decreased as the impeller diameter was increased. The blade width, however, had no effect on the mean drop diameter. For impellers A4 and A3, the mean drop diameters were of the same order of magnitude. The diameter-to-width ratio of these two impellers is 4.10 and 8.00 respectively; a factor of approximately two. A cross-plot of these data indicates that the mean drop diameter is proportional to the impeller diameter to the minus three-halves power, i.e.,

$$d = c/L^{1.5}. \qquad (20)$$

It is of interest to note here that since the mean drop diameter is independent of blade width, and power consumption is directly proportional to blade width, the same degree of dispersion could be obtained with a decrease in power consumption at a given impeller diameter and impeller speed by reducing the blade width of the impeller. This may be explained as due to the fact that the power required for agitation is controlled by the volume swept out by the impeller, whereas the Reynolds number, which is a measure of the intensity of turbulence, is controlled only by the peripheral velocity of the impeller.

Effect of Baffling: The observed mean drop diameters for unbaffled agitation were, on the average, a factor of 1.5 times greater than those obtained for baffled agitation. The power consumption for baffled agitation is a factor of approximately 3 greater than that for the unbaffled case. These data indicate that the power required to obtain a given degree of dispersion is nearly the same for either condition of agitation.

For the unbaffled runs, 100 ml. samples were taken from the bottom center of the tank during agitation, and the resulting volume fraction of the dispersed phase observed. These data were used to calculate "mixing index" values (ratio of local volume fraction of one phase, usually the light phase, to the mean volume fraction of that phase) which are given in Tables 13-17. These samples are not entirely representative of the tank contents, but do give a relative indication of the uniformity of mixing.

Effect of Other Variables; Steps Toward a General Correlation: In attempting to find a general correlation for the effect of all the variables studied, it was found convenient to use d_o, the mean drop diameter extrapolated to zero volume fraction of dispersed phase. Use of this quantity simplified the correlation problem by separating out the effect of coalescence.

In order to test the validity of a previous correlation (11), a plot of d_o/L versus Weber number, $N^2L^3\rho/\sigma$, was made. This plot was made using values of d_o obtained by Equations (6) and (19), and in both cases there was a scatter of the data through a factor of four. Additional data showed that the exponent on L for such a plot should be 5/2, indicating that the Weber number should be combined with another dimensionless number. The Froude number, N^2L/g, was introduced as a trial factor, but it only increased the scatter between systems.

Log-log and semi-log plots were also made of d_o versus σ/ρ. Plots were also prepared of d_o versus $\Delta\rho/\rho_c$. No significant trend in the data was observed in these plots.

Since it was found earlier that viscosity did not appreciably affect the extent of interfacial area formed (11), the present investigation did not cover a wide range of this variable. Correction factors such as the viscosity ratio were tried, however, in an attempt to bring the data together into a general correlation. These correction factors were too small to shift the data significantly. Since the previous study did not include cases in which both the continuous and the dispersed phase had high viscosities,

it remains possible that a system of this type might show some effect.

A completely general correlation has not yet been found, and there is evidently an effect of the physical variables that has not yet been resolved. For each of the systems so far investigated in detail, the following equation, which is a combination of Equations (15), (17), (19), and (20), applies:

$$A = (\text{constant})\, 6\phi\, e^{-2.0(\phi)^{0.5}} N L^{1.5} \qquad (21)$$

The constants are not dimensionless, and vary both with the system and the extent of baffling.

VI. CONCLUSIONS

1. Light transmissions provide a rapid and accurate measurement of interfacial area for two-phase liquid emulsions in which each phase is separately transparent.
2. For stirred-tank systems of different sizes but similar proportions, the interfacial area depends on the stirring speed, impeller diameter, and volume fraction of dispersed phase. The effect of interfacial tension, mean density, density difference, and viscosities of the fluids has not yet been resolved. Mean drop diameters were found to be approximately 1.5 times larger in the case of unbaffled tanks.
3. Power requirements for the agitation of two-phase liquid systems were found to be identical with those for a homogeneous liquid of equal mean density.

4. The interfacial area appears unaffected by the width of the impeller. This suggests that drop diameter is controlled by the highest intensity of turbulence reached at any point in the tank. If this observation is correct, it indicates that the impeller width and number of blades may be reduced to the minimum values that will still give homogeneous dispersion (100 percent mixing index). Thus, the dependence of mixing index upon impeller design and speed is a possible future study that is economically important.
5. Viscosity effects were not investigated in the present work, and they are also recommended as a subject for future study. The dissimilar behavior of gas-liquid systems suggests that high values of μ_d/ρ_d may give slow rates of bursting. Williams (28) has found that the slopes of log d versus $(\phi)^{0.5}$ are steeper for gas-liquid systems, indicating a more rapid coalescence. Since white oil-water and other liquid-liquid systems also have high values of μ_d/ρ_d, but probably very low coalescence rates, the effect of volume fraction on mean drop diameter in such systems should be investigated. It is already known that the rates of approach to steady state in these systems are very low.

This work was performed under the auspices of the U.S. Atomic Energy Commission.

VII. NOMENCLATURE

Latin Letter Symbols

a = constant

A = specific area = total interfacial area per unit volume, cm^2/cm^3

A2, A3, A4 = small tank impellers; see Table 1

b = slope of plot of log d versus $(\phi)^{0.5}$

B1, B2, B3, B4 = large tank impellers; see Table 1

C_v = velocity gradient, u/x, in which drop exists, sec^{-1}

d = mean drop diameter, cm.

d_o = mean drop diameter for $\phi = 0$, cm.

$F = 2C_v\mu d/\sigma$

Fr = Froude number $= N^2L/g$, dimensionless

e = base of natural logarithms

g = gravitational constant

I = light transmission through emulsion

I_o = light transmission through continuous phase alone

I_o/I = light extinction ratio

k = proportionality constant

L = impeller diameter, cm. and in.

m = refractive index ratio, n_d/n_c

n_c = refractive index (n_D^{20}) of continuous phase at sodium D line

n_d = refractive index (n_D^{20}) of dispersed phase at sodium D line

N = stirring speed, rpm or rps

P = power, ft-lbs/min

Latin Letter Symbols (cont'd)

P_o = power number = $Pg/\rho N^3 \cdot 1/L^5$, dimensionless

P_w = power number = $Pg/\rho N^3 \cdot 1/L^4W$, dimensionless

R = torque arm, ft

Re = Reynolds number = $NL^2\rho/\mu$, dimensionless

R_1 = radius of external cylinder in Clay's model apparatus

T = torque, ft - lbs. (Wherever "T" occurs in tables, dimensions should read "ft - lbs" rather than "lbs".)

W = blade width, cm and in

We = Weber number = $N^2L^3\rho/\sigma$, dimensionless

Greek Letter Symbols

β = proportionality constant in Equation (1) relating I_o/I and A

μ_c = viscosity of continuous phase, gm/cm-sec

μ_d = viscosity of dispersed phase, gm/cm-sec

ρ_c = density of continuous phase, gm/cc

ρ_d = density of dispersed phase, gm/cc

ρ = mean density for drops = $0.4\rho_d + 0.6\rho_c$, gm/cc

σ = interfacial tension, dynes/cm

ϕ = volume fraction of dispersed phase, cc/cc

VIII. BIBLIOGRAPHY

1. Castleman, R. A., Jr., Bur. Standards J. Research, 6, 369 (1931)
2. Clay, P. H., Proc. Acad. Sci. Amsterdam, 43, 852, 979 (1940)
3. Cooper, C. M., Fernstrom, G. A., and Miller, S. A., Ind. Eng. Chem., 36, 504 (1944)
4. Foust, H. G., Mack, D. E., Rushton, J. H., Ind. Eng. Chem., 36, 517 (1944)
5. Haenlein, A., T. M. No. 659, Nat. Advisory Comm. Aeronaut., (1931)
6. Hixson, A. W. and Baum, S. J., Ind. Eng. Chem., 33, 478 (1941)
7. Hixson, A. W. and Crowell, J. H., Ibid, 23, 923, 1002, 1160 (1931)
8. Hixson, A. W. and Luedeke, V. D., Ibid, 29, 927 (1937)
9. Hixson, A. W. and Tenney, A. H., Trans. Am. Inst. Chem. Engrs., 31, 113 (1935)
10. Hixson, A. W. and Wilkins, G. A., Ind. Eng. Chem., 25, 1196 (1933)
11. Langlois, G. E., Ph. D. Chemistry Thesis, University of California (1952)
12. Lee, D. W. and Spencer, R. C., T. R. No. 454 Nat. Advisory Comm. Aeronaut., (1933)
13. Lewis, H. C., Edwards, D. G., Goglia, M. J., Rice, R. I., and Smith, L. W., Ind. Eng. Chem., 40, 67 (1948)
14. Long, Ray, M. S. Chem. Eng. Thesis, University of California (1949)

15. Mack, D. E. and Kroll, A. E., Chem. Eng. Progr., 44, 189 (1948)

16. Mack, D. E. and Marriner, R. A., Chem. Eng. Progr., 45, 545 (1949)

17. Merrington, A. C. and Richardson, E. G., Proc. Phys. Soc., 59, 1 (1947)

18. Miller, S. A. and Mann, C. A., Trans. Am. Inst. Chem. Engrs., 40, 709 (1944)

19. Nukiyama, S. and Tanasawa, Y., Trans. Soc. Mech. Engrs., (Japan), 4, No. 14, 86 (1938)

20. Ibid, No. 15, 138 (1938); 5, No. 18, 63 (1939)

21. Ibid, 6, No. 22, II-7 (1940); 6, No. 23, II-8, (1940)

22. Olney, R. B., and Carlson, G. J., Chem. Eng. Progr., 43, 473 (1947)

23. Rushton, J. H., Chem. Eng. Progr., 48, 33 (1952); 48, 95 (1952)

24. Rushton, J. H., Costich, E. W., and Everett, H. J., Ibid, 46, 395 (1950)

25. Rushton, J. H., Private Communication

26. Taylor, G. I., Proc. Roy. Soc., A146, 501 (1934)

27. White, A. M., and Summerford, A. D., Ind. Eng. Chem., 25, 1025 (1933); 26, 82 (1934)

28. Williams, G., Private Communication

APPENDIX I

Figures 1 - 31

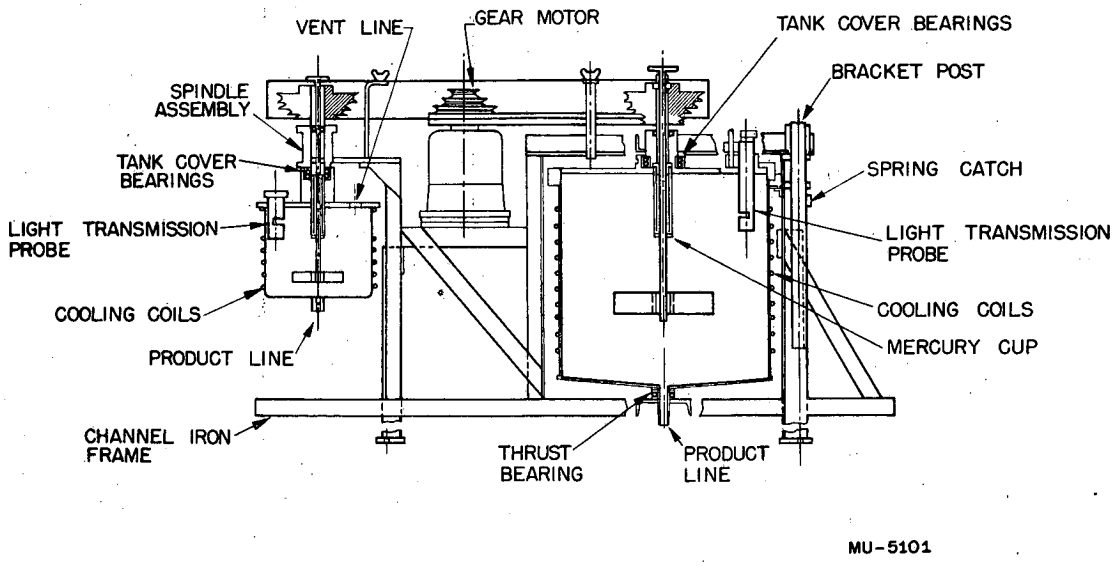

Figure 1. Assembly Drawing of Tanks.

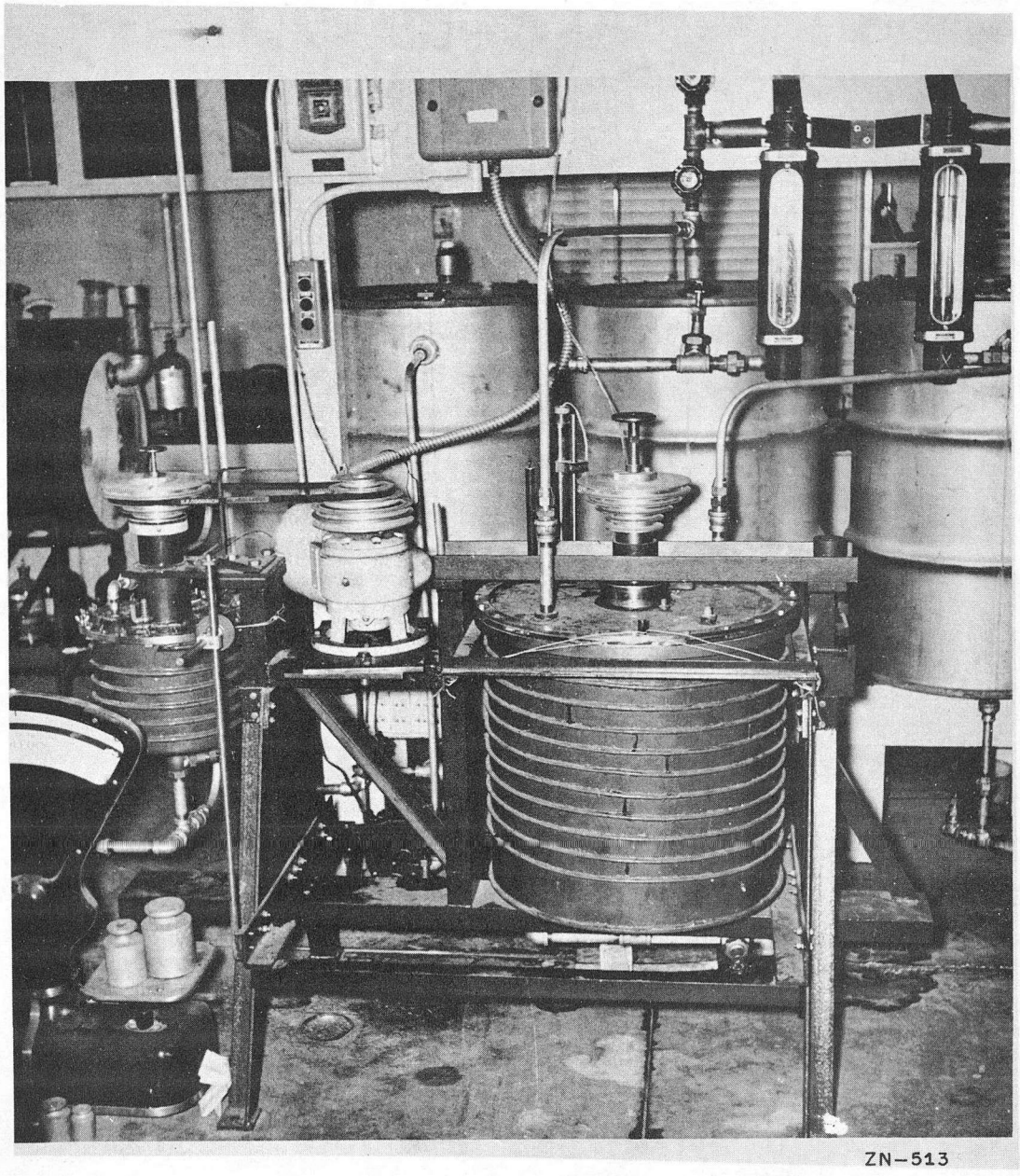

Figure 2. Photograph of Tanks.

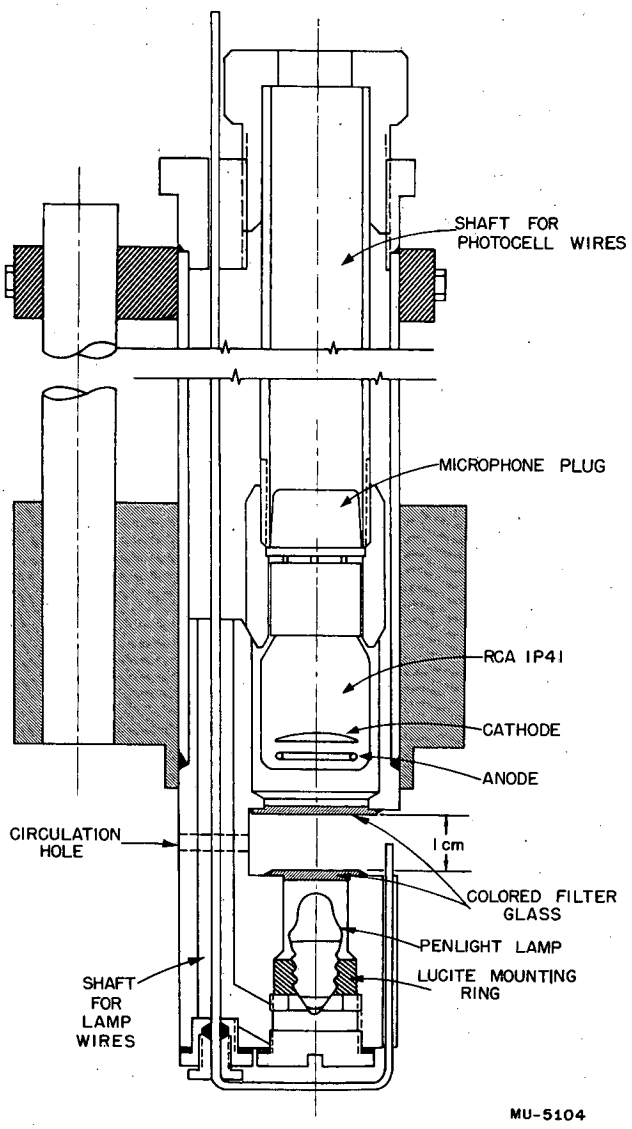

Figure 3. Assembly Drawing of Light Transmission Probe.

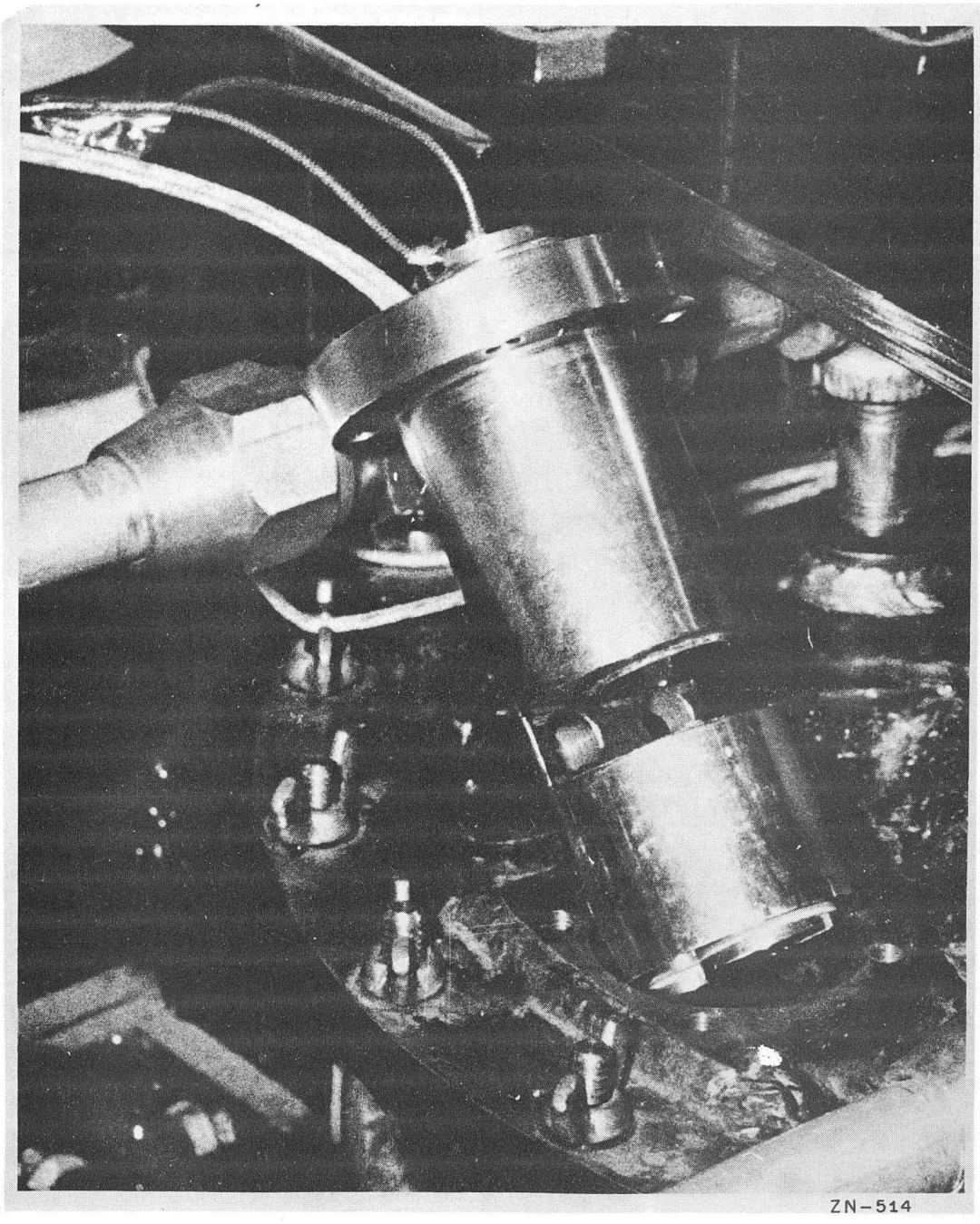

Figure 4. Photograph of Small Tank Light Transmission Probe.

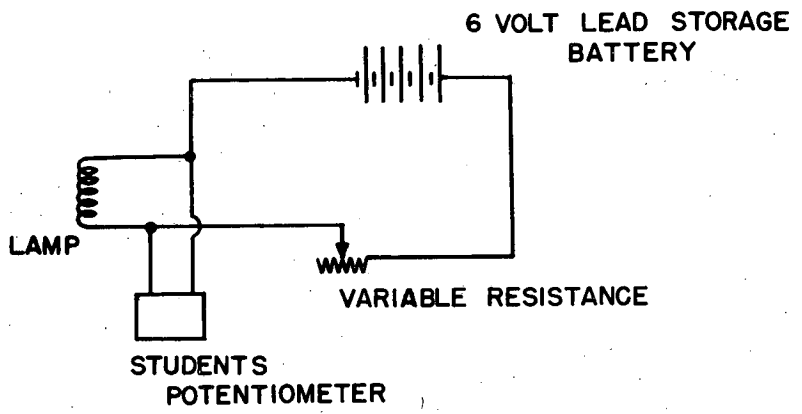

Figure 5. Penlight Lamp Circuit.

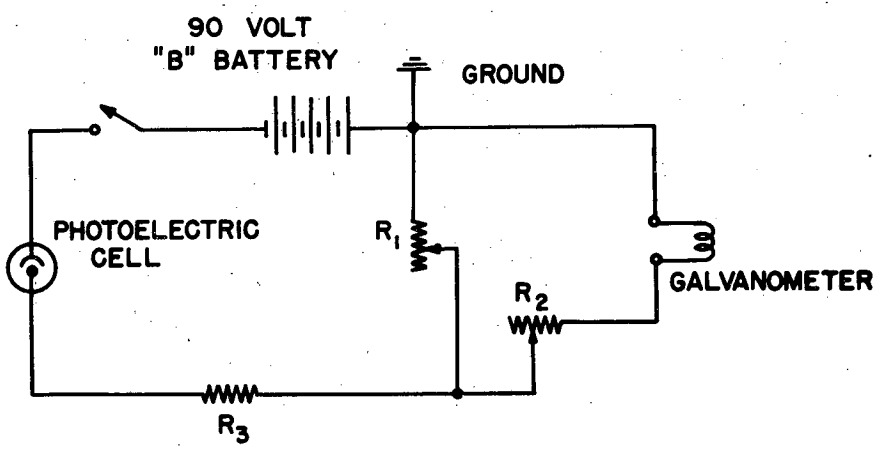

Figure 6. Photoelectric Cell Circuit.

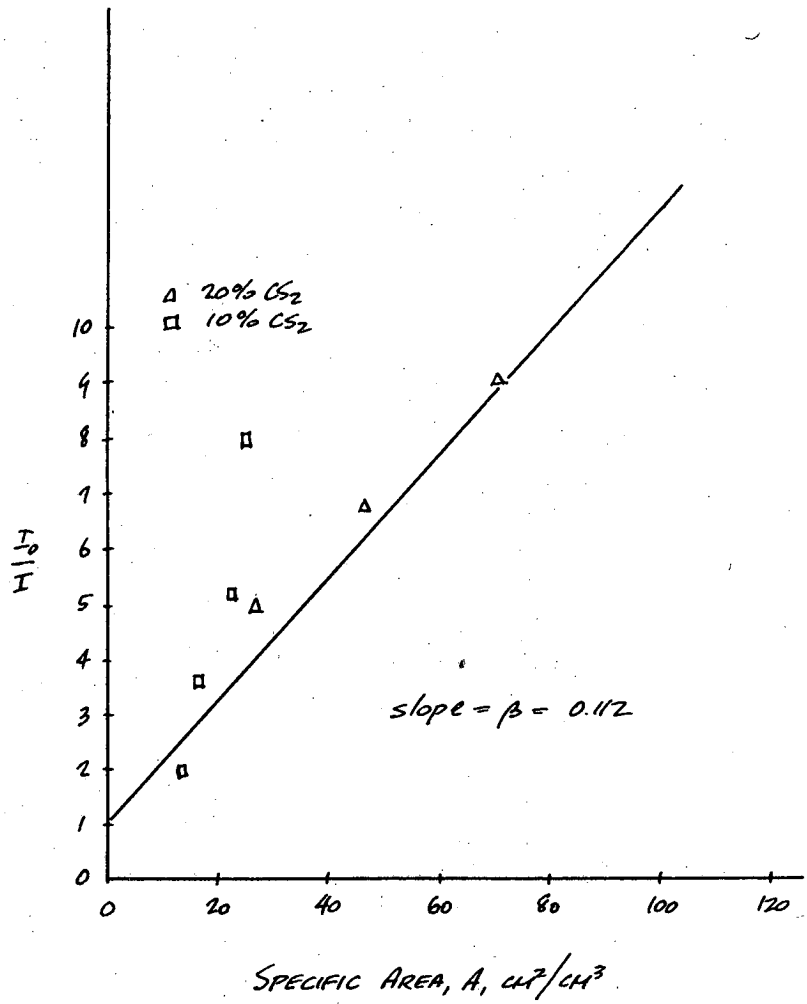

FIGURE 7: PLOT OF $\frac{I_o}{I}$ VS SPECIFIC AREA FOR THE SYSTEM: CS_2-H_2O

MU-4715

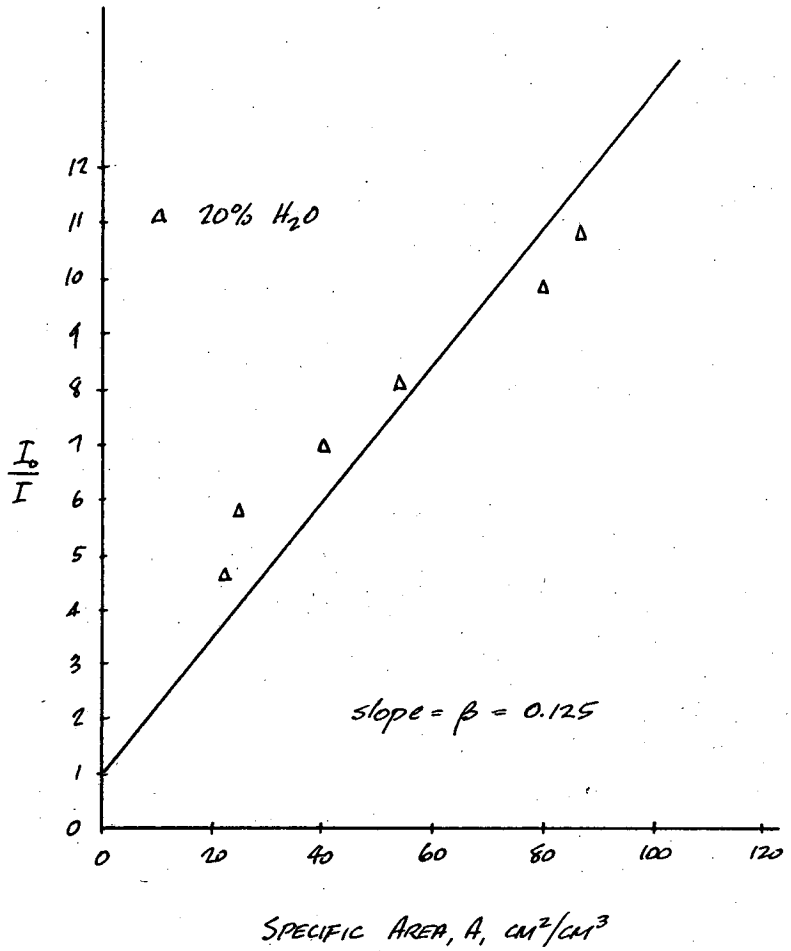

FIGURE 8: PLOT OF $\frac{I_o}{I}$ VS SPECIFIC AREA FOR THE SYSTEM: H_2O-CS_2

MU-4716

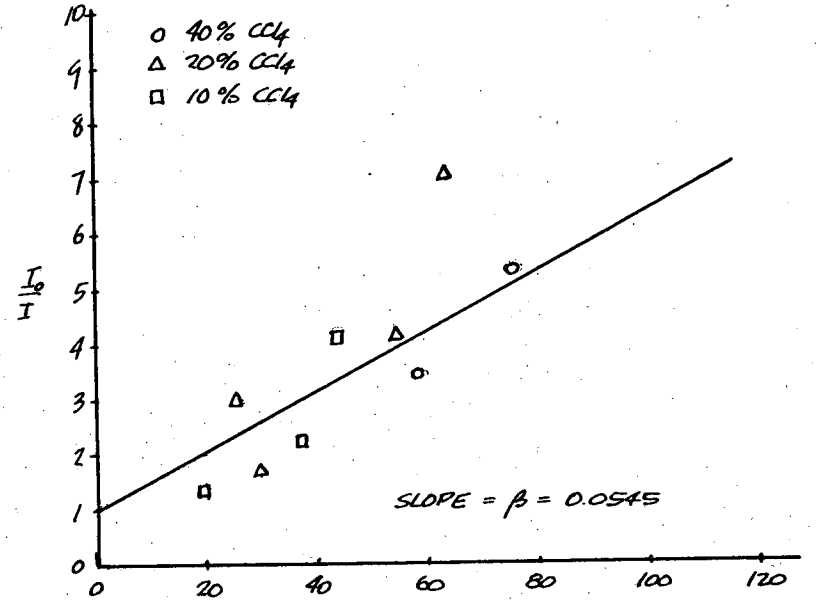

FIGURE 9: PLOT OF $\frac{I_0}{I}$ VS SPECIFIC AREA FOR THE SYSTEM: CCl_4-H_2O

MU-4717

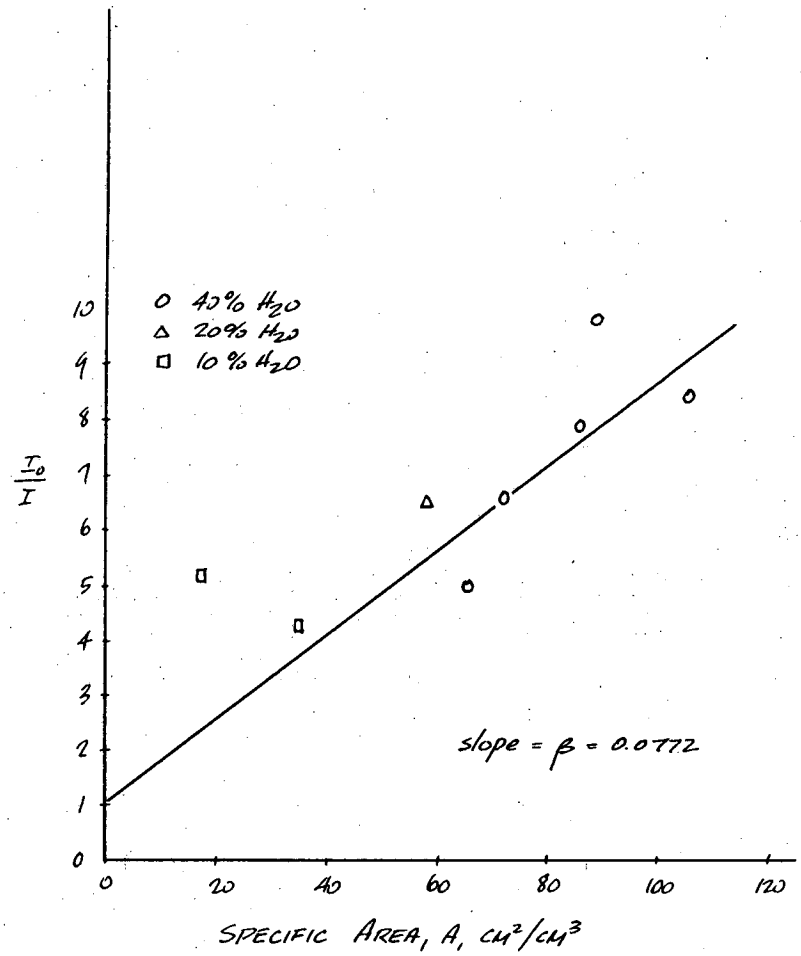

FIGURE 10: PLOT OF $\frac{I_o}{I}$ VS SPECIFIC AREA FOR THE SYSTEM: H_2O-CCl_4

MU-4718

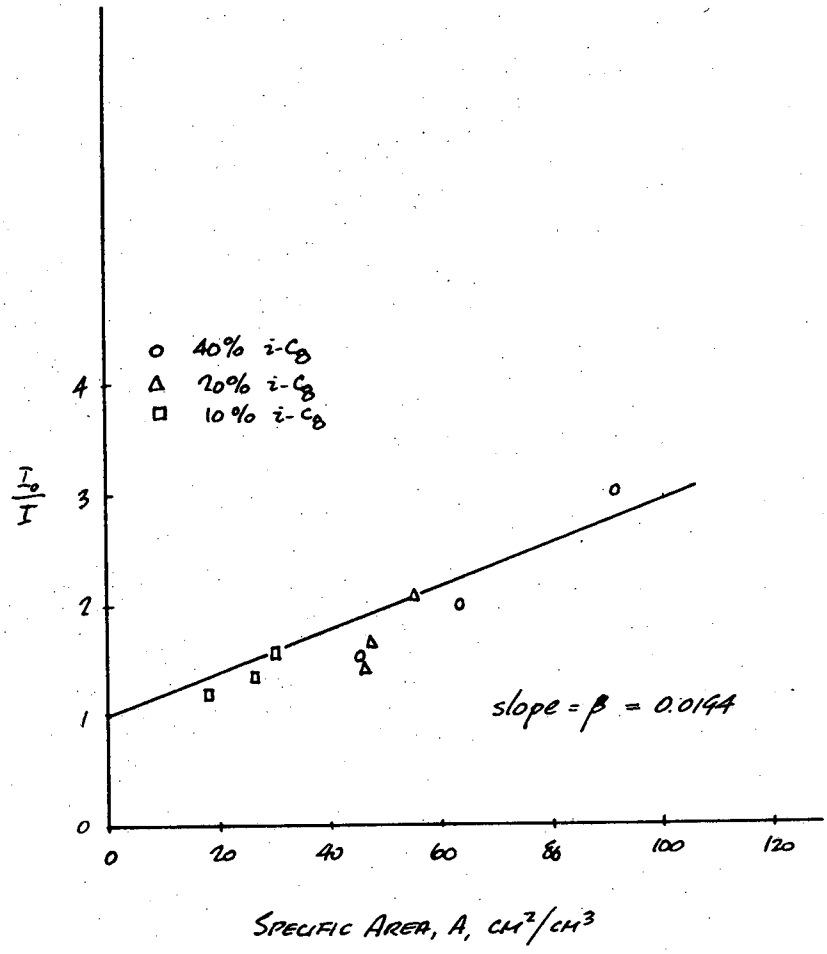

FIGURE 11: PLOT OF $\frac{I_0}{I}$ VS SPECIFIC AREA FOR THE SYSTEM: iC_8-H_2O

MU-4719

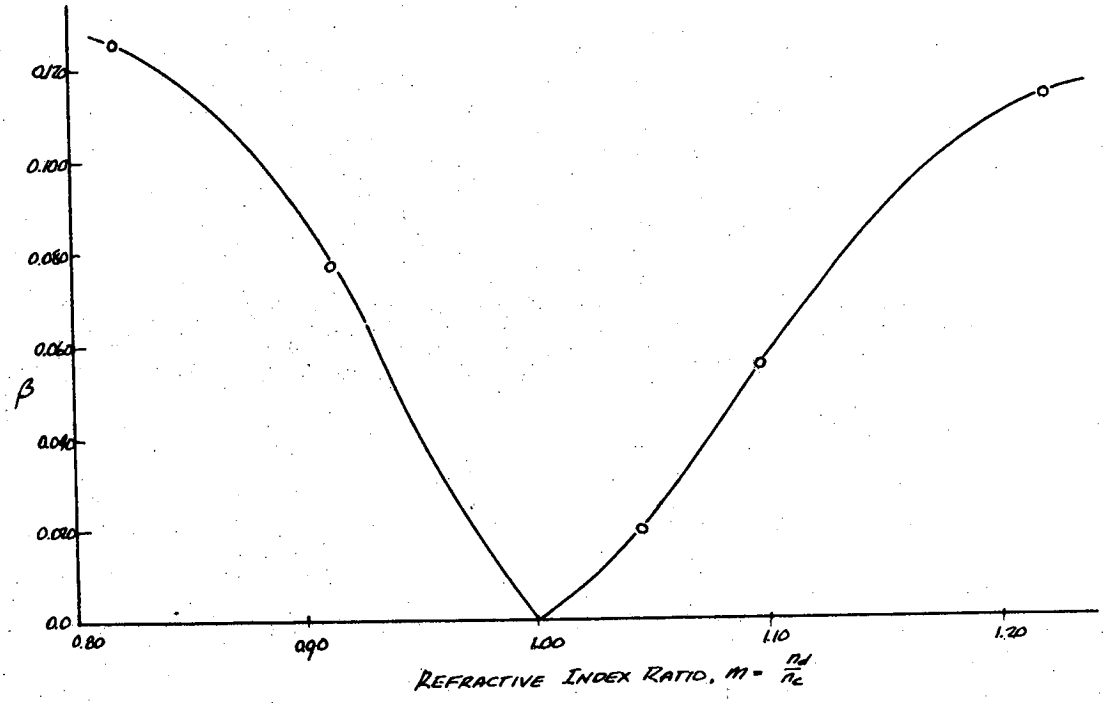

FIGURE 12: PLOT OF β VS REFRACTIVE INDEX RATIO

MU-4720

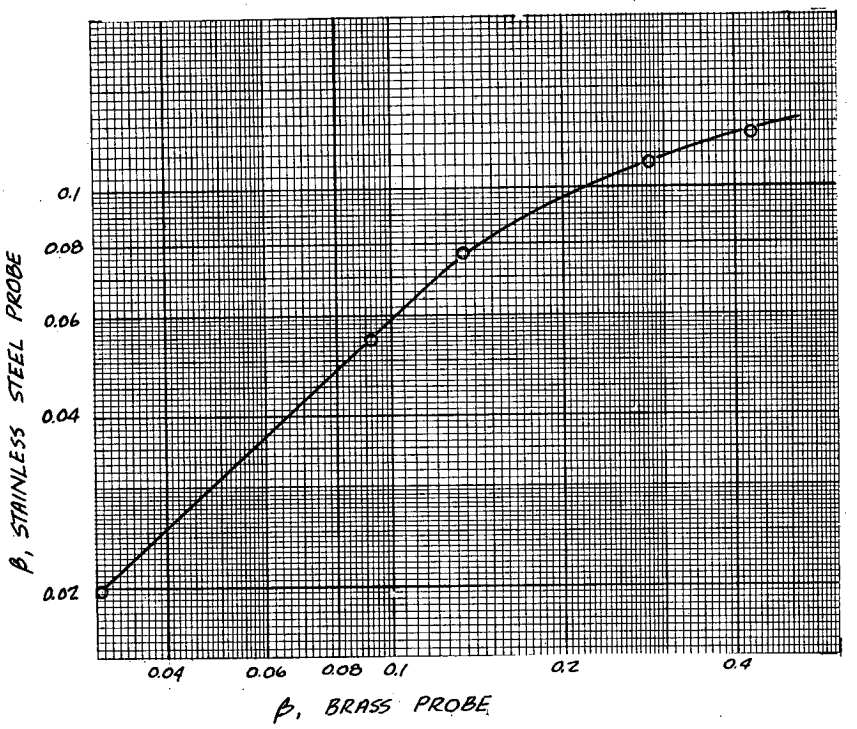

FIGURE 13: CROSS PLOT OF β VALUES FOR LIGHT TRANSMISSION PROBES

MU-4721

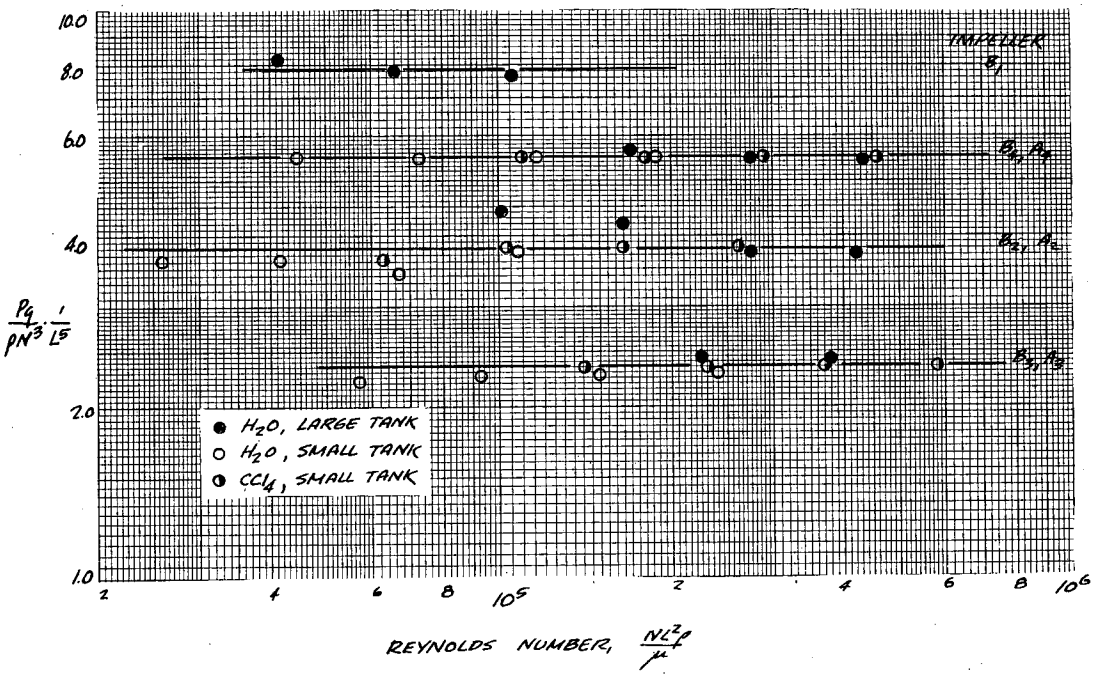

FIGURE 14: EFFECT OF IMPELLER GEOMETRY ON SINGLE-PHASE POWER, BAFFLED TANK

MU-4722

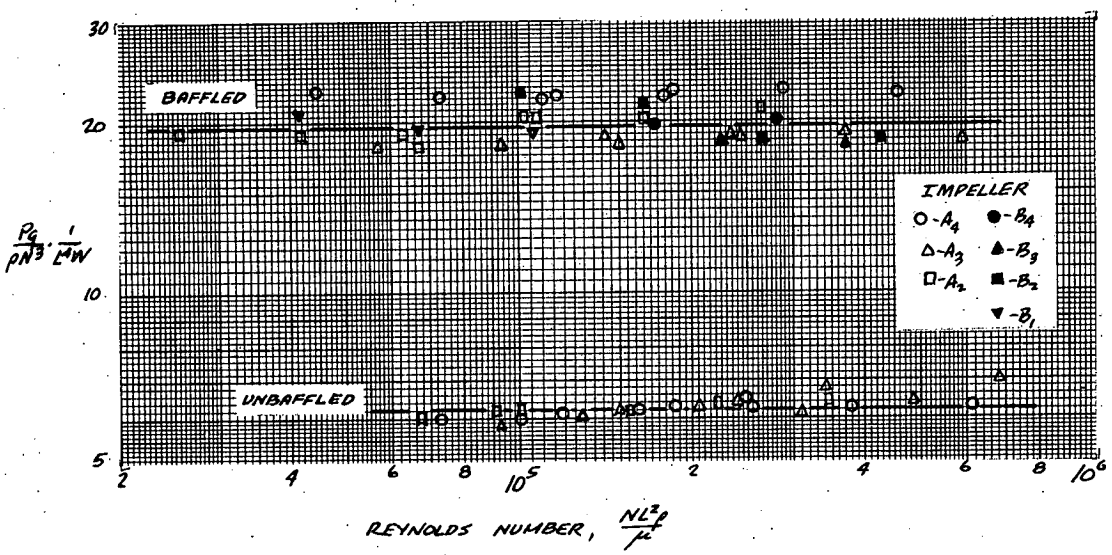

FIGURE 15: GENERALIZED CORRELATION OF SINGLE-PHASE SYSTEM POWER

MU-4723

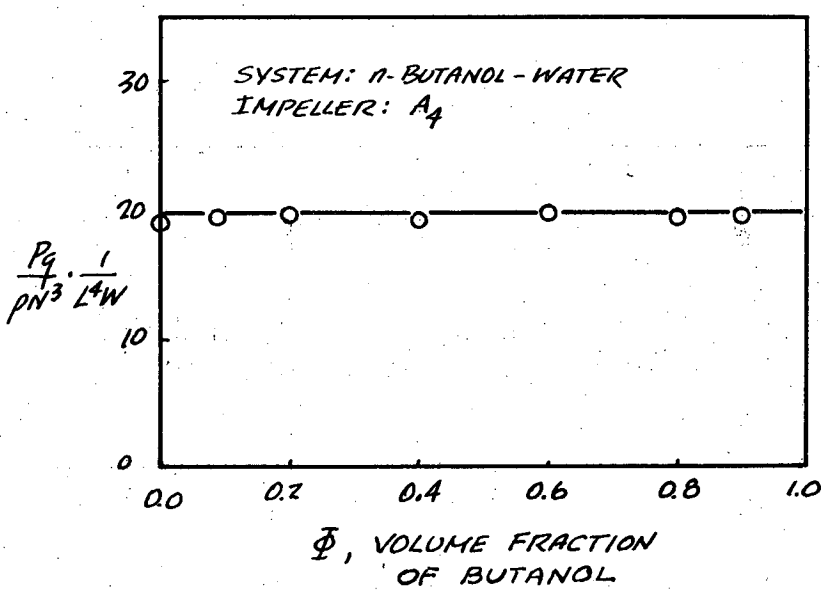

FIGURE 16: EFFECT OF VOLUME FRACTION ON POWER

MU-4724

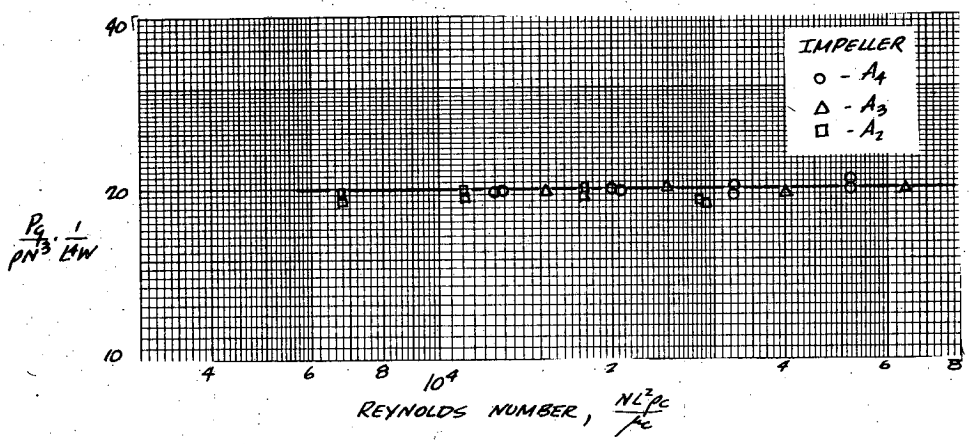

FIGURE 17: TWO-PHASE POWER AT LOW REYNOLDS NUMBERS, WATER DISPERSED IN BUTANOL

MU-4725

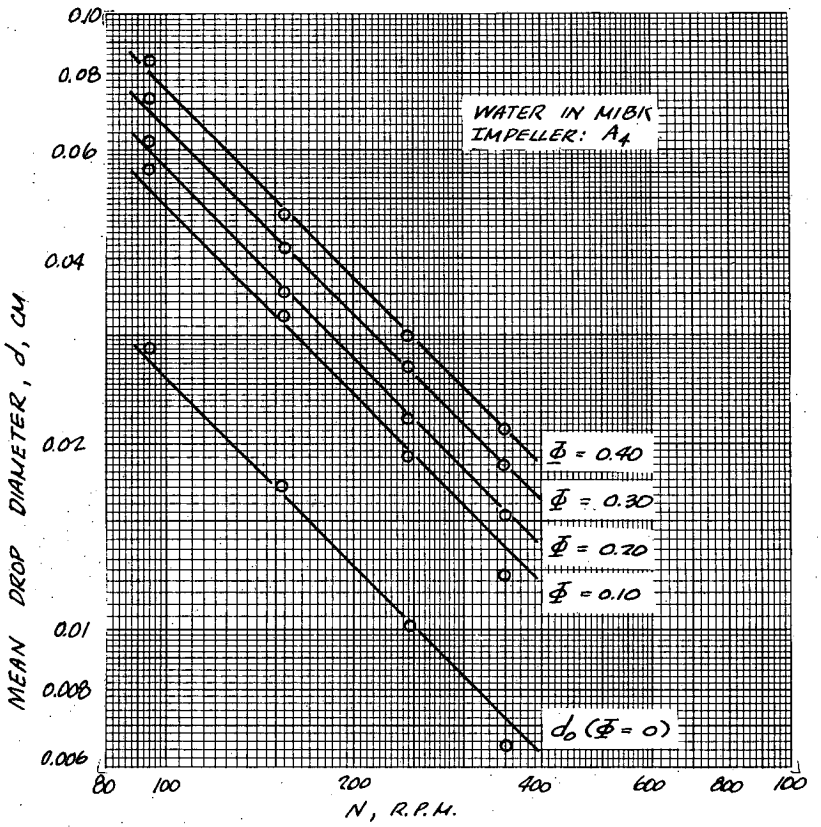

FIGURE 18: EFFECT OF STIRRING SPEED ON MEAN DROP DIAMETER

MU-4726

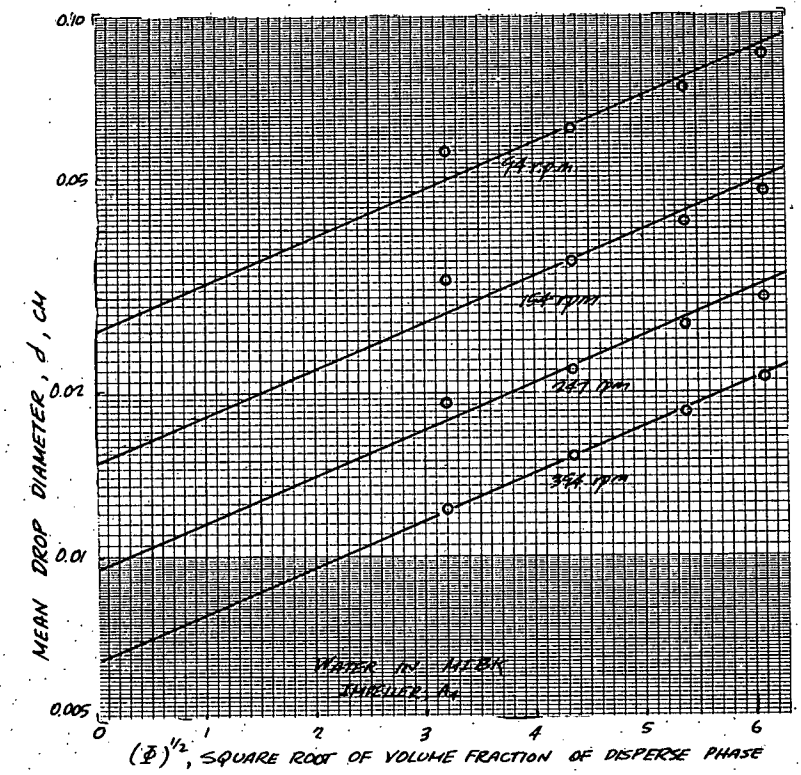

FIGURE 19: EFFECT OF VOLUME FRACTION ON MEAN DROP DIAMETER

MU-4727

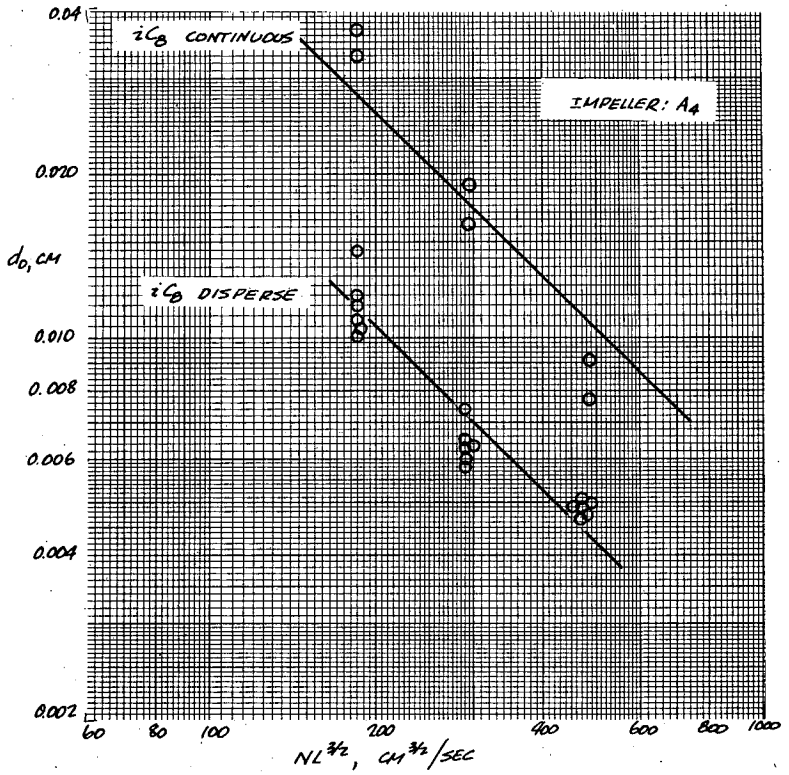

FIGURE 20: DROP DIAMETER CORRELATION FOR THE SYSTEM: ISO-OCTANE - WATER

MU-4728

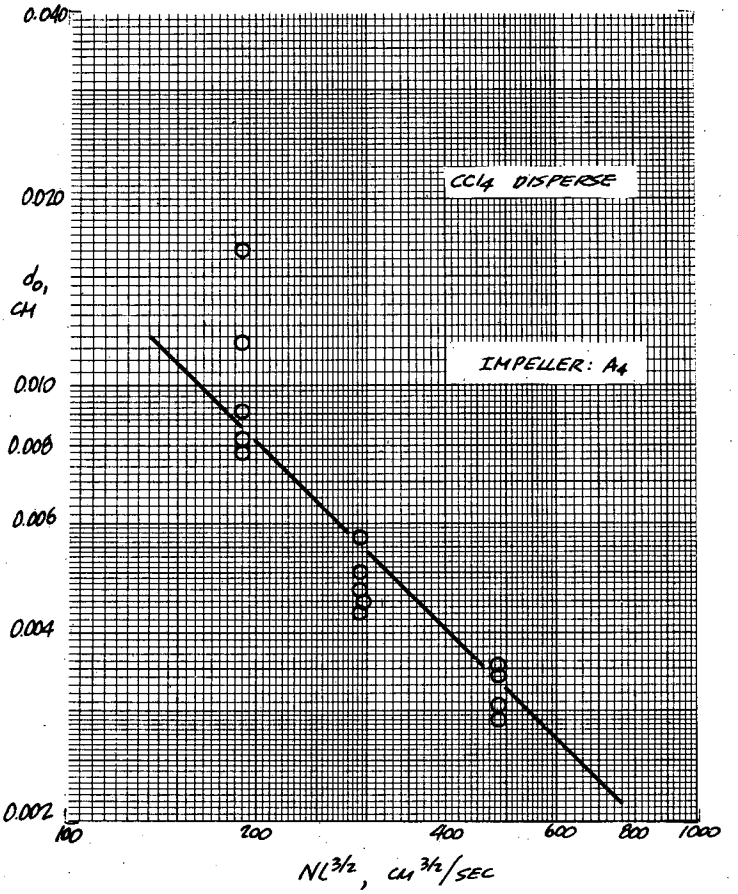

FIGURE 21: DROP DIAMETER CORRELATION FOR THE SYSTEM: CARBON TETRACHLORIDE - WATER

MU-4729

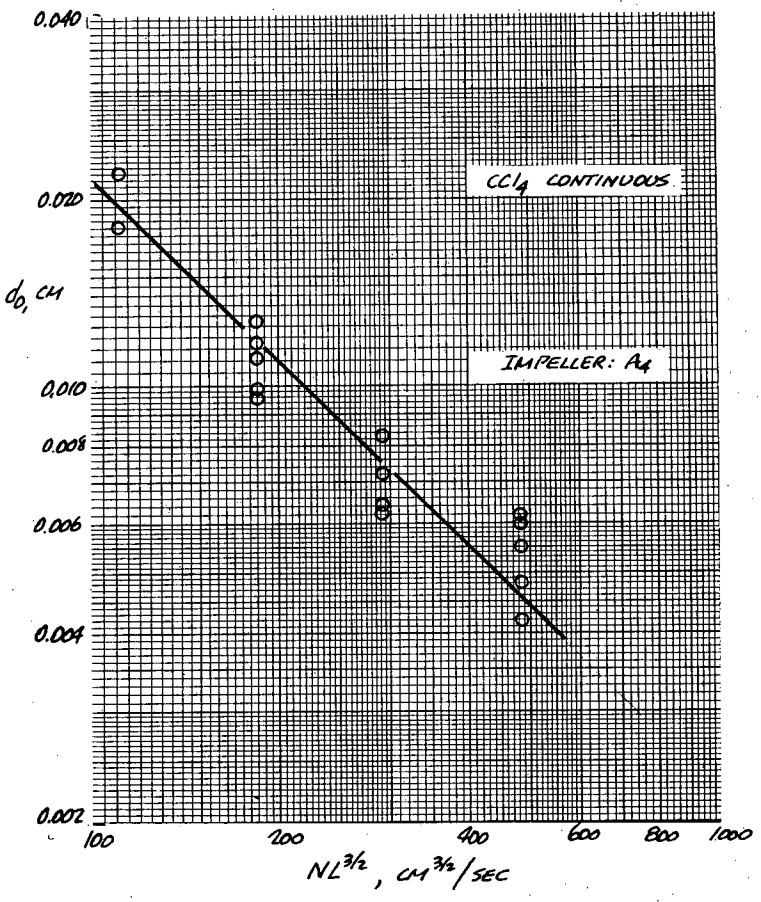

FIGURE 22: DROP DIAMETER CORRELATION FOR THE SYSTEM: CARBON TETRACHLORIDE-WATER

MU-4730

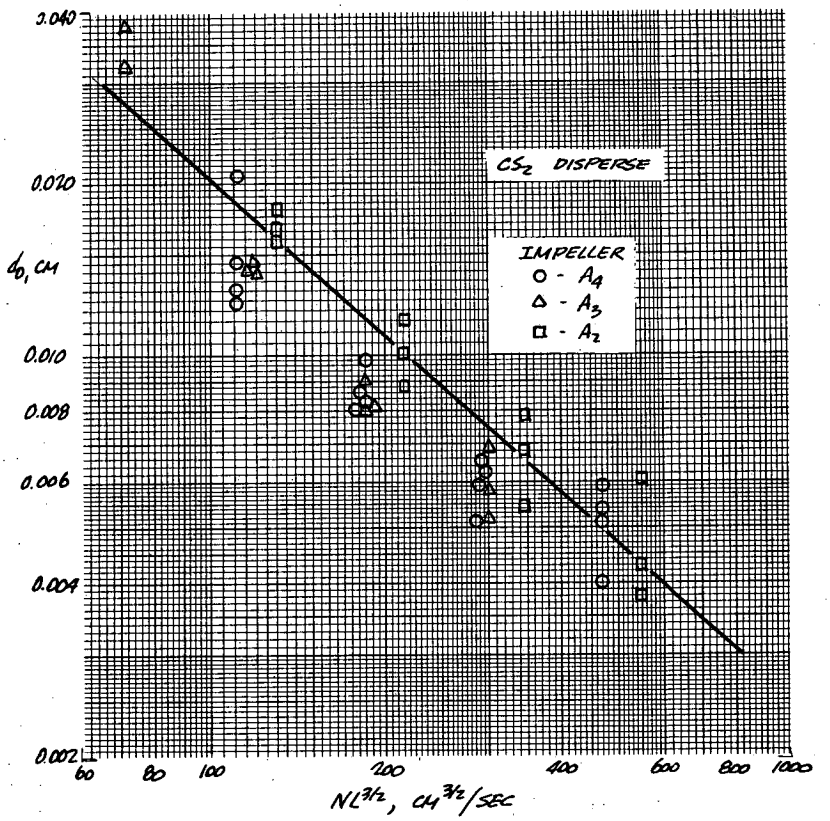

FIGURE 23: DROP DIAMETER CORRELATION FOR THE SYSTEM: CARBON DISULFIDE – WATER

MU-4731

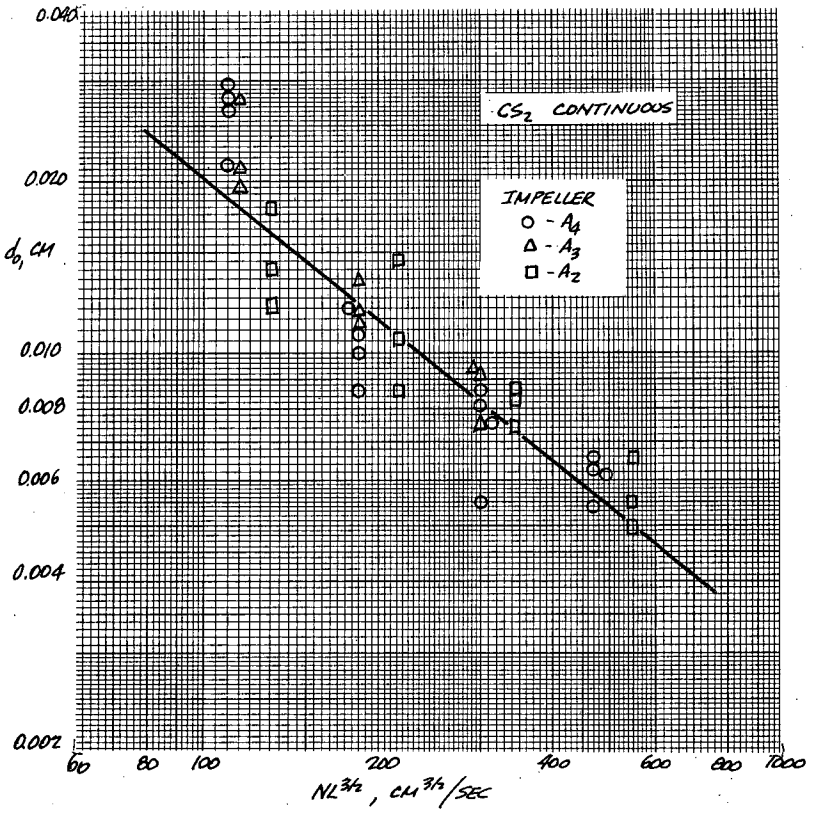

FIGURE 24: DROP DIAMETER CORRELATION FOR THE SYSTEM: CARBON DISULFIDE - WATER

MU-4732

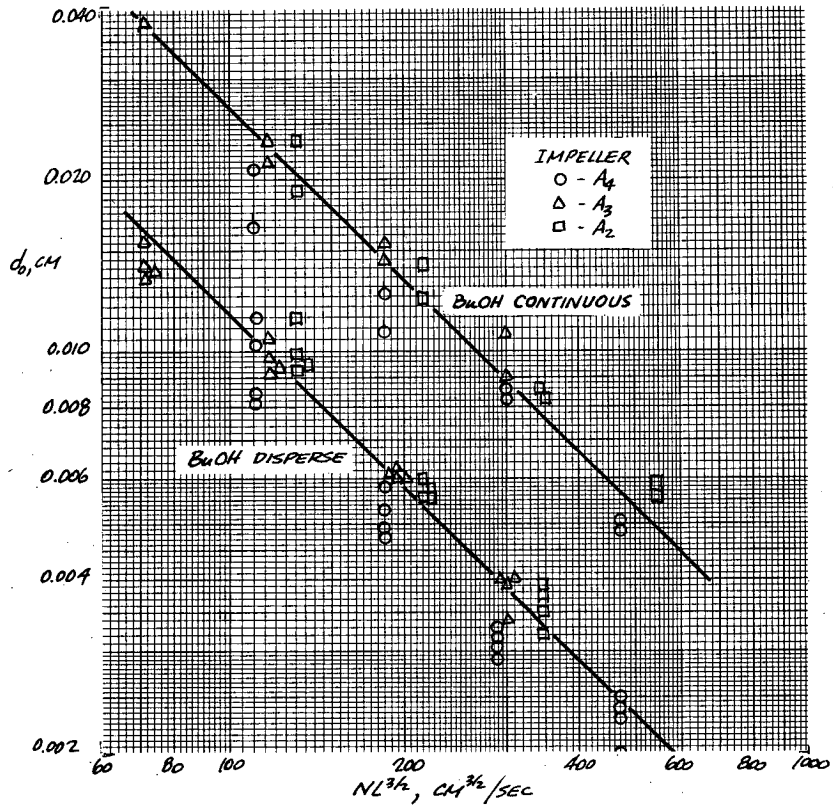

FIGURE 25: DROP DIAMETER CORRELATION FOR THE SYSTEM n-BUTANOL-WATER

MU-4733

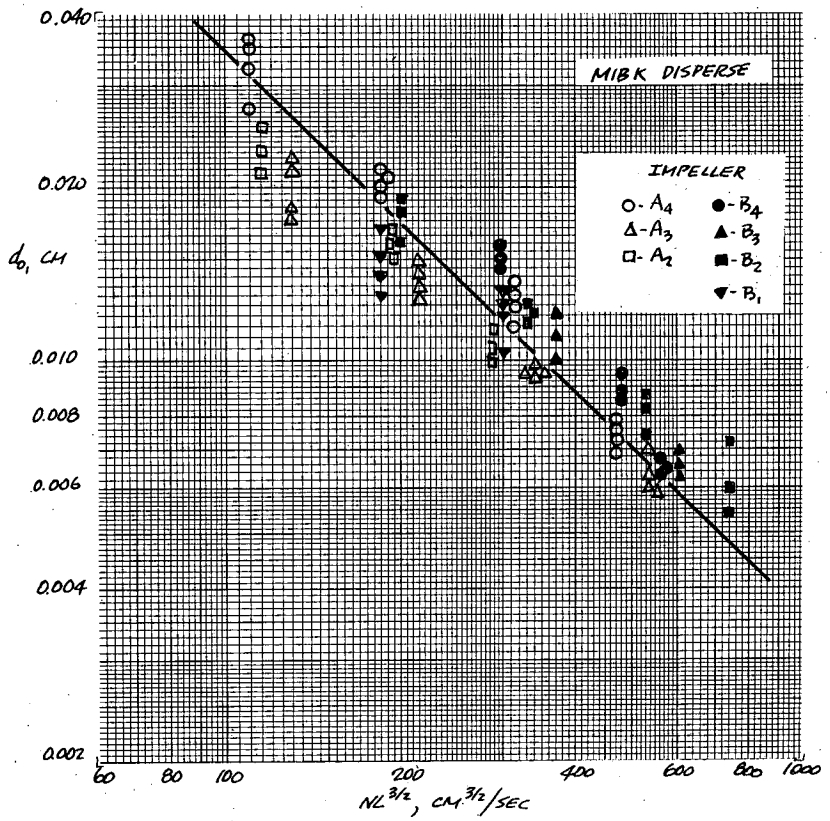

FIGURE 26: DROP DIAMETER CORRELATION FOR THE SYSTEM: METHYL ISOBUTYL KETONE - WATER

MU-4734

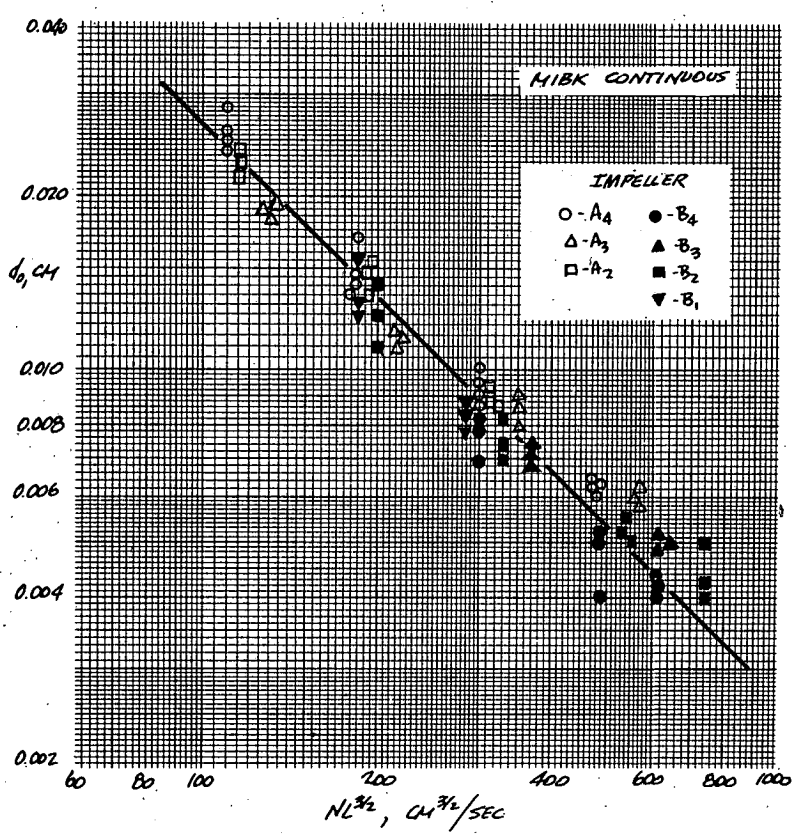

FIGURE 27: DROP DIAMETER CORRELATION FOR THE SYSTEM: METHYL ISOBUTYL KETONE - WATER

MU-4735

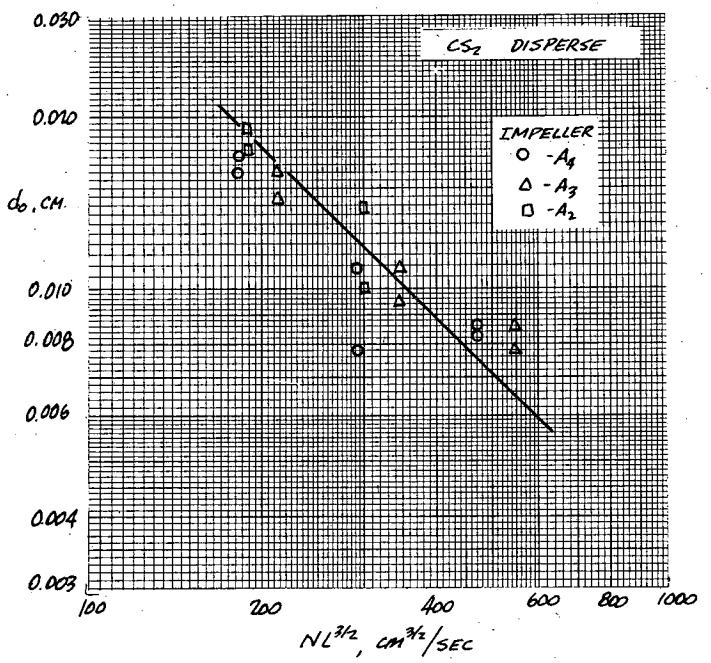

FIGURE 28: DROP DIAMETER CORRELATION FOR THE SYSTEM CARBON DISULFIDE - WATER, UNBAFFLED

MU-4736

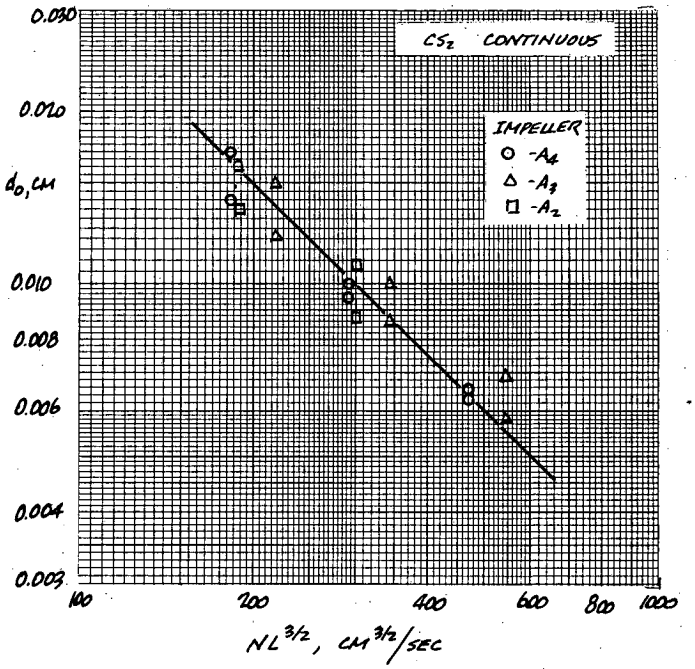

FIGURE 29: DROP DIAMETER CORRELATION FOR THE SYSTEM: CARBON DISULFIDE - WATER, UNBAFFLED

MU-4737

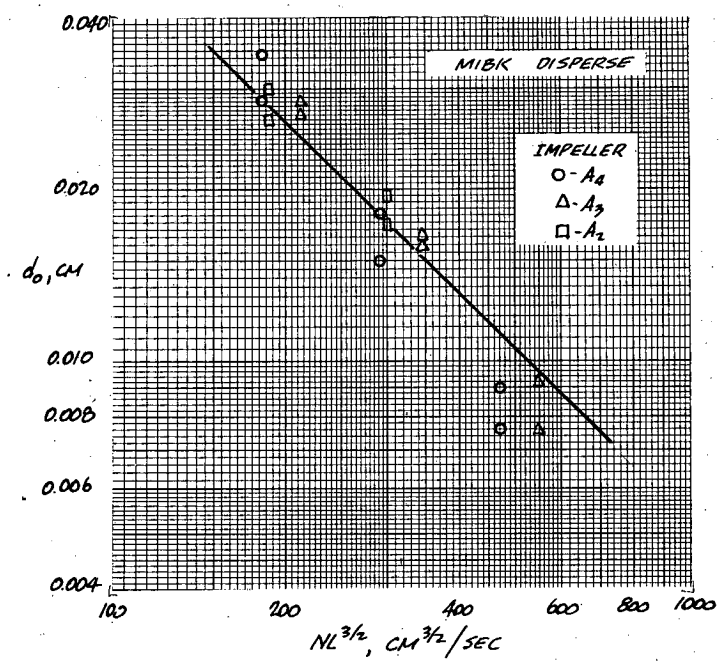

FIGURE 30: DROP DIAMETER CORRELATION FOR THE SYSTEM: METHYL ISOBUTYL KETONE - WATER, UNBAFFLED

MII-4738

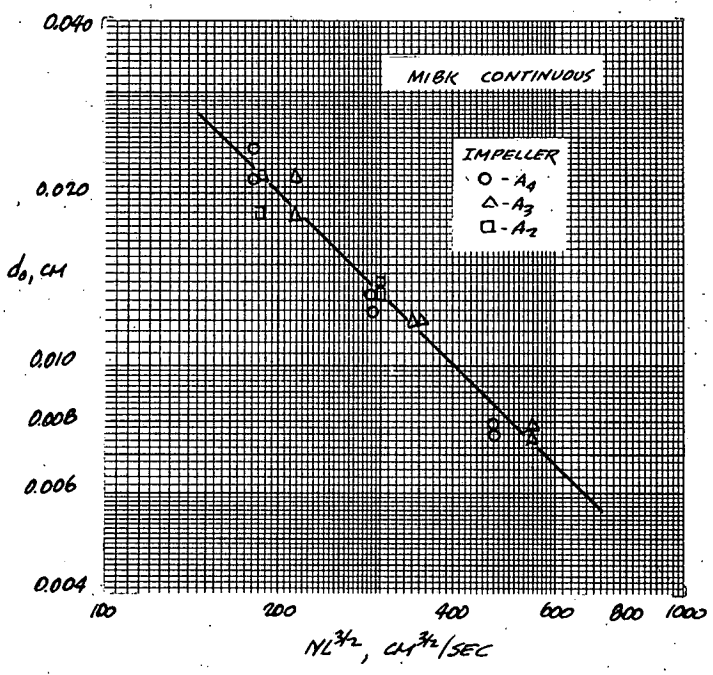

FIGURE 31: DROP DIAMETER CORRELATION FOR THE SYSTEM: METHYL ISOBUTYL KETONE - WATER, UNBAFFLED

MU-4739

APPENDIX II

Tables 1 - 19

Table 1

Dimensions of Mixing Apparatus
(Inches)

	10" Tank (A)	20" Tank (B)
Tank Height	8.87	20.00
Tank Diameter	10.35	20.00
Baffle Width	1.00	2.00
Number of Baffles	4.	4.
Diameter of Impeller #1		5.00
Width of Impeller #1		2.00
Diameter of Impeller #2	5.00	10.00
Width of Impeller #2	0.94	2.00
Diameter of Impeller #3	7.50	15.00
Width of Impeller #3	0.94	2.00
Diameter of Impeller #4	6.77	13.00
Width of Impeller #4	1.65	3.72
Number of Blades on all Impellers	4.	4.

Table 2

Physical Properties of Liquids Used in Mixing Studies[1]

Liquid	Refractive Index n_{20}^{D}	Density gm/cc	Viscosity cp	Interfacial Tension[2] dynes/cm
Water	1.3330	0.998	1.000	---
Carbon tetrachloride	1.4601	1.595	0.990	39.9
Carbon disulfide	1.6273	1.265	0.378	35.2
Iso-octane (2,2,4-trimethyl pentane)	1.3910	0.693	0.517	46.5
Methyl isobutyl ketone	1.3940	0.800	0.585	9.6
n-Butanol	1.3991	0.806	2.950	2.4

[1]All properties measured at 20° C.

[2]Interfacial tension with water as the other phase.

Table 3

Photographic and Light Transmission Data

System[1]	Refractive Index Ratio m	Volume Fraction of Dispersed Phase ϕ	Specific Area, A cm^2/cm^3	Light Ratio $\frac{I_o}{I}$	Stirring Speed N rpm
H_2O-CCl_4	0.9130	0.400	87.8	9.84	400
	0.9130	0.400	85.1	7.93	255
	0.9130	0.400	65.1	5.00	140
	0.9130	0.400	71.5	6.60	189
	0.9130	0.400	105.0	8.45	289
	0.9130	0.200	58.3	6.52	228
	0.9130	0.100	34.4	4.31	225
	0.9130	0.100	17.7	5.17	288
CCl_4-H_2O	1.0956	0.396	59.2	3.48	102
	1.0956	0.396	75.0	5.40	147
	1.0956	0.202	25.4	2.95	128
	1.0956	0.202	30.0	1.70	101
	1.0956	0.202	54.5	4.20	158
	1.0956	0.202	63.5	7.10	266
	1.0956	0.099	19.4	1.35	114
	1.0956	0.099	37.0	2.25	158
	1.0956	0.099	43.5	4.15	244
i-C_8-H_2O	1.0439	0.399	44.8	1.55	102
	1.0439	0.399	63.1	2.00	141
	1.0439	0.399	91.3	3.05	246
	1.0439	0.201	36.0	1.46	111
	1.0439	0.201	55.0	2.18	198
	1.0439	0.201	47.2	1.72	144
	1.0439	0.098	17.7	1.23	110
	1.0439	0.098	26.4	1.37	150
	1.0439	0.098	30.1	1.56	204

[1] Dispersed phase listed first.

Table 3 (Cont'd)

System[1]	Refractive Index Ratio m	Volume Fraction of Dispersed Phase ϕ	Specific Area, A cm^2/cm^3	Light Ratio $\frac{I_o}{I}$	Stirring Speed N rpm
CS_2-H_2O	1.2208	0.090	13.8	1.98	98
	1.2208	0.090	16.2	3.58	137
	1.2208	0.090	21.7	5.21	189
	1.2208	0.090	24.5	7.97	288
	1.2208	0.200	26.6	4.98	100
	1.2208	0.200	46.2	6.82	140
	1.2208	0.200	70.2	9.12	203
H_2O-CS_2	0.8192	0.204	21.7	4.65	104
	0.8192	0.204	24.4	5.81	122
	0.8192	0.204	79.6	9.90	300
	0.8192	0.204	53.7	8.16	191
	0.8192	0.204	40.1	6.99	150
	0.8192	0.204	86.9	10.91	400

[1]Dispersed phase listed first

Table 4

Single-Phase Power Data

Liquid	Impeller Number	L/W	rpm	T lbs.	P_o	P_w	$Re \cdot 10^{-4}$
H_2O	A2	5.33	94	0.073	3.62	19.31	2.54
			154	0.194	3.58	19.09	4.16
			247	0.471	3.38	18.03	6.70
			394	1.365	3.85	20.53	10.60
H_2O	A2	8.00	94	0.346	2.27	18.16	5.69
			154	0.926	2.26	18.08	9.32
			247	2.398	2.28	18.24	14.95
			394	6.265	2.34	18.72	23.80
H_2O	A4	4.10	94	0.448	5.52	22.65	4.45
			154	1.190	5.46	22.40	7.30
			247	2.070	5.48	22.48	11.70
H_2O	B1	2.50	154	0.250	8.33	20.83	4.14
			247	0.600	7.77	19.43	6.64
			394	1.500	7.63	19.08	10.60
H_2O	B2	5.00	94	1.623	4.54	22.70	10.10
			154	4.070	4.24	21.20	16.50
			247	9.183	3.72	18.60	26.50
			345	17.810	3.70	18.50	42.20
H_2O	B3	7.50	94	6.722	2.48	18.60	22.60
			151	16.578	2.37	17.78	37.00
H_2O	B4	3.52	94	7.510	5.68	19.97	16.90
			151	19.460	5.70	20.04	28.00
CCl_4	A2	5.33	94	0.116	3.64	19.41	6.28
			154	0.329	3.84	20.48	10.30
			247	0.849	3.85	20.53	16.50
			394	2.230	3.98	21.23	26.30
CCl_4	A3	8.00	94	0.569	2.35	18.80	14.10
			154	1.506	2.32	18.56	23.10
			247	3.917	2.34	18.72	37.10
			394	9.801	2.30	18.40	59.00
CCl_4	A4	4.10	94	0.710	5.49	22.53	11.00
			154	1.920	5.53	22.69	18.00
			247	4.970	5.56	22.81	28.90
			394	12.500	5.50	22.57	46.00

Table 4 (Cont'd)

Single-Phase Power Data for Unbaffled Conditions

Liquid	Impeller Number	$\frac{L}{W}$	rpm	T^1 lbs.		P^1 w	
				w.	w.o.	w.	w.o.
H_2O	A2	5.33	154	--	--	--	--
			247	0.16	0.11	6.12	4.21
			394	0.42	0.33	6.31	4.96
H_2O	A3	8.00	154	0.30	0.21	5.85	4.09
			247	0.82	0.59	6.24	4.49
			394	2.19	1.67	6.54	4.99
H_2O	A4	4.10	154	0.32	0.22	6.02	4.14
			247	0.84	0.61	6.14	4.47
			394	2.23	1.71	6.42	4.92
MIBK	A2	5.33	247	0.13	0.10	6.22	4.79
			394	0.33	0.26	6.20	4.89
MIBK	A3	8.00	154	0.25	0.17	6.10	4.15
			247	0.66	0.48	6.28	4.56
			394	1.82	1.27	6.81	4.75
MIBK	A4	4.10	154	0.26	0.19	6.11	4.46
			247	0.68	0.54	6.22	4.94
			394	1.75	1.34	6.30	4.82
CS_2	A2	5.33	247	0.21	0.16	6.36	4.85
			394	0.55	0.43	6.54	5.12
CS_2	A3	8.00	154	0.40	0.32	6.17	4.94
			247	1.09	0.83	6.56	5.00
			394	2.07	2.57	7.01	4.89
CS_2	A4	4.10	154	0.46	0.34	6.84	5.06
			247	1.07	0.85	6.20	4.92
			394	2.76	2.16	6.29	4.92
CCl_4	A4	4.10	154	0.54	0.42	6.37	4.96
			247	1.37	1.07	6.29	4.91
			394	3.53	2.77	6.39	5.01

[1] w. - power measured with light transmission probe in tank.
w.o. - power measured without light transmission probe in tank.

Table 5

Drop Diameter and Power Data for the System:
Iso-octane dispersed-Water continuous

Impeller Number	Volume Fraction $i\text{-}C_8$	N rpm	$\frac{I_o}{I}$	d cm.	d_o cm.	$\frac{Nd_oL^{1.5}}{cm^{2.5}/sec}$	T lbs.	P_w
A4	0.087	154	1.392	0.0258	0.0142	2.60	1.117	21.62
		247	1.758	0.0134	0.0074	2.17	2.968	22.33
		394	2.148	0.0088	0.0049	2.30	7.414	21.93
	0.200	154	1.794	0.0293	0.0120	2.20	1.054	21.71
		247	2.522	0.0153	0.0063	1.85	2.811	21.16
		394	2.853	0.0126	0.0051	2.39	7.297	22.38
	0.400	154	2.148	0.0406	0.0115	2.11	0.948	20.36
		247	3.053	0.0227	0.0064	1.88	2.557	21.35
		394	3.702	0.0172	0.0049	2.30	6.577	21.58
	0.443	154	2.260	0.0409	0.0108	1.978	0.926	20.19
		247	3.164	0.0238	0.0063	1.85	2.497	21.17
		394	3.867	0.0180	0.0048	2.25	6.351	21.16
	0.520	154	2.425	0.0425	0.0101	1.85	0.885	19.84
		247	3.471	0.0245	0.0058	1.70	2.349	20.47
		394	4.124	0.0194	0.0046	2.156	6.236	21.36
	0.600	154	2.425	0.0490	0.0104	1.90	0.868	20.05
		247	3.540	0.0275	0.0059	1.73	2.296	20.61
		394	3.963	0.0236	0.0050	2.34	5.908	20.84
	H_2O							
A4	0.092	154	1.257	0.0602	0.0327	5.99	0.808	21.16
		247	1.439	0.0352	0.0191	5.61	2.250	22.90
		394	1.924	0.0167	0.0091	4.26	5.697	22.79
	0.223	154	1.384	0.0952	0.0370	6.78	0.850	21.03
		247	1.903	0.0414	0.0161	4.73	2.306	22.18
		394	2.902	0.0197	0.0077	3.61	5.892	22.27

Table 6

Drop Diameter and Power Data for the System:
Carbon tetrachloride-water

Impeller Number	Volume Fraction CCl_4	N rpm	$\frac{I_o}{I}$	d cm.	d_o cm.	$\frac{Nd_oL^{1.5}}{cm^{2.5}/sec}$	T lbs.	P w
A4	0.087	154	2.347	0.0211	0.0117	2.14	--	--
		247	4.681	0.0077	0.0043	1.26	--	--
		394	6.377	0.0053	0.0029	1.36	--	--
	0.196	154	3.911	0.0220	0.0091	1.67	1.224	20.61
		247	6.822	0.0110	0.0045	1.32	3.172	20.77
		394	8.622	0.0084	0.0035	1.64	8.191	21.07
	0.298	154	5.027	0.0242	0.0082	1.50	1.310	20.96
		247	8.011	0.0139	0.0047	1.38	3.475	21.62
		394	10.370	0.0104	0.0035	1.64	8.903	21.77
	0.398	154	5.677	0.0278	0.0079	1.45	1.367	20.82
		247	8.980	0.0163	0.0046	1.35	3.58	21.20
		394	11.892	0.0119	0.0034	1.59	9.101	21.18
	H_2O							
A4	0.087	94	2.238	0.0326	0.0181	2.02	0.680	22.28
		154	3.255	0.0178	0.0099	1.81	1.683	20.55
		247	4.590	0.0112	0.0062	1.82	5.032	19.13
		394	6.393	0.0075	0.0042	1.97	10.520	19.62
	0.194	94	2.672	0.0537	0.0223	2.49	0.613	20.95
		154	4.839	0.0234	0.0097	1.78	1.742	22.18
		247	6.832	0.0154	0.0064	1.88	4.460	22.07
		394	8.689	0.0116	0.0048	2.25	11.134	21.66
	0.308	154	5.234	0.0337	0.0111	1.32	1.590	21.22
		247	7.521	0.0218	0.0072	2.12	4.212	21.85
		394	9.421	0.0169	0.0055	2.58	10.589	21.49
	0.412	154	5.491	0.0425	0.0117	2.14	1.517	21.18
		247	7.851	0.0278	0.0077	2.26	3.966	21.52
		394	9.835	0.0216	0.0060	2.81	9.855	21.02
	0.459	154	5.296	0.0495	0.0128	2.34	1.502	21.41
		247	7.650	0.0320	0.0083	2.44	3.947	21.87
		394	10.056	0.0235	0.0061	2.86	9.726	21.18

Table 7

Drop Diameter and Power Data for the System:
Carbon disulfide dispersed-Water continuous

Impeller Number	Volume Fraction CS_2	N rpm	$\frac{I_o}{I}$	d cm.	d_o cm.	$\frac{Nd_oL^{1.5}}{cm^{2.5}}$ sec	T lbs.	P_w
A4	0.090	94	2.612	0.0375	0.0206	2.30	0.390	19.26
		154	4.375	0.0179	0.0098	1.80	1.163	21.40
		247	7.292	0.0096	0.0053	1.56	3.115	22.28
		394	9.211	0.0073	0.0040	1.87	7.913	22.25
	0.195	94	4.730	0.0351	0.0145	1.62	0.395	18.99
		154	7.479	0.0202	0.0083	1.52	1.170	20.96
		247	10.174	0.0143	0.0059	1.73	3.143	21.89
		394	11.667	0.0123	0.0051	2.39	8.059	22.06
	0.297	94	6.177	0.0386	0.0130	1.45	0.410	19.22
		154	8.838	0.0254	0.0086	1.58	1.201	20.98
		247	11.824	0.0184	0.0062	1.82	3.101	21.05
		394	13.462	0.0161	0.0054	2.53	8.179	21.82
	0.399	94	7.114	0.0438	0.0123	1.38	0.415	19.85
		154	10.294	0.0288	0.0082	1.50	1.200	21.38
		247	12.681	0.0230	0.0065	1.91	3.200	22.16
		394	13.889	0.0208	0.0059	2.76	8.190	22.29
A3	0.084	94	3.017	0.0280	0.0157	2.05	0.380	19.49
		154	4.564	0.0158	0.0088	1.88	1.065	20.35
		247	6.846	0.0097	0.0054	1.85	2.563	19.04
		394	9.368	0.0067	0.0038	2.08	6.392	18.66
	0.200	94	4.139	0.0428	0.0175	2.28	0.395	19.66
		154	5.742	0.0283	0.0116	2.48	1.070	19.85
		247	7.970	0.0193	0.0079	2.70	2.609	19.04
		394	10.076	0.0148	0.0061	3.33	6.521	18.48
	0.394	94	5.742	0.0558	0.0160	2.084	0.405	19.22
		154	8.476	0.0354	0.0101	2.16	1.103	19.50
		247	12.130	0.0238	0.0068	2.33	2.678	18.41
		394	18.600	0.0150	0.0043	2.35	6.806	18.38
A2	0.098	94	2.106	0.0596	0.0319	2.26	0.075	19.33
		154	3.510	0.0262	0.0140	1.63	0.190	18.24
		247	5.424	0.0149	0.0080	1.49	0.511	19.07
		394	7.786	0.0097	0.0052	1.55	1.355	19.90

Table 7 (Cont'd)

Drop Diameter and Power Data for the System:
Carbon disulfide dispersed-Water continuous

Impeller Number	Volume Fraction CS_2	N rpm	$\frac{I_o}{I}$	d cm.	d_o cm.	$\frac{Nd_oL^{1.5}}{cm^{2.5}}$ sec	T lbs.	P_w
	0.198	94	2.452	0.0916	0.0378	2.68	0.075	18.84
		154	4.838	0.0347	0.0143	1.66	0.200	18.72
		247	7.783	0.0196	0.0081	1.51	0.516	18.72
		394	10.529	0.0140	0.0058	1.72	1.395	19.95
	0.398	154	6.393	0.0496	0.0140	1.63	0.205	18.27
		247	9.421	0.0318	0.0090	1.68	0.531	18.39
		394	11.933	0.0245	0.0069	2.05	1.422	19.36

Table 8

Drop Diameter and Power Data for the System:
Water dispersed-Carbon disulfide continuous

Impeller Number	Volume Fraction H_2O	N rpm	$\frac{I_o}{I}$	d cm.	d_o cm.	$\frac{Nd_o L^{1.5}}{cm^{2.5}}$ sec	T lbs.	P w
A4	0.087	94	2.354	0.0482	0.0267	2.99	0.515	20.97
		154	5.215	0.0155	0.0086	1.58	1.485	22.53
		247	7.623	0.0099	0.0055	1.62	3.826	22.62
		394	9.118	0.0080	0.0044	2.06	9.524	22.07
	0.198	94	3.875	0.0517	0.0214	2.39	0.495	20.64
		154	7.154	0.0241	0.0100	1.83	1.379	21.42
		247	9.208	0.0181	0.0075	2.20	3.688	22.28
		394	10.941	0.0149	0.0062	2.91	9.162	21.75
	0.349	94	3.720	0.0962	0.0296	3.31	0.460	19.84
		154	8.378	0.0355	0.0109	1.99	1.314	21.11
		247	10.941	0.0263	0.0081	2.38	3.552	22.19
		394	13.881	0.0203	0.0063	2.95	8.805	21.61
	0.471	94	4.133	0.1127	0.0286	3.20	0.445	19.74
		154	8.455	0.0474	0.0120	2.20	1.297	21.43
		247	11.482	0.0337	0.0086	2.53	3.389	21.77
		394	15.246	0.0248	0.0063	2.95	8.497	21.45
A3	0.087	94	3.957	0.0220	0.0122	1.59	0.425	17.94
		154	4.429	0.0191	0.0106	2.26	1.177	18.51
		247	5.813	0.0136	0.0075	2.57	3.052	18.66
		394	8.455	0.0088	0.0049	2.68	7.822	18.79
	0.197	94	4.429	0.0431	0.0178	2.32	0.420	18.15
		154	5.167	0.0354	0.0146	3.12	1.133	18.25
		247	7.949	0.0211	0.0087	2.98	2.914	18.24
		394	10.220	0.0160	0.0066	3.60	7.384	18.17
	0.392	94	7.154	0.0478	0.0137	1.79	0.415	18.72
		154	10.941	0.0296	0.0085	1.81	1.101	18.52
		247	14.091	0.0225	0.0065	2.23	2.801	18.32
		394	16.316	0.0192	0.0055	3.00	7.108	18.27
A2	0.087	154	2.842	0.0354	0.0196	2.28	0.235	18.64
		247	4.064	0.0213	0.0118	2.20	0.638	19.67
		394	5.788	0.0136	0.0075	2.23	1.704	20.65

Table 8 (Cont'd)

Drop Diameter and Power Data for the System:
Water dispersed-Carbon disulfide continuous

Impeller Number	Volume Fraction H_2O	N rpm	$\frac{I_o}{I}$	d cm.	d_o cm.	$\frac{Nd_o L^{1.5}}{cm^{2.5}/Sec}$	T lbs.	P_w
A2	0.200	154	3.205	0.0680	0.0278	3.23	0.225	18.29
		247	5.618	0.0325	0.0133	2.48	0.614	19.40
		394	7.640	0.0226	0.0092	2.74	1.639	20.35
	0.403	154	4.988	0.0758	0.0213	2.47	0.215	18.28
		247	8.304	0.0413	0.0116	2.16	0.582	19.24
		394	10.053	0.0334	0.0094	2.79	1.578	20.50

Table 9

Drop Diameter and Power Data for the System:
n-Butanol dispersed-Water continuous

Impeller Number	Volume Fraction BuOH	N rpm	$\frac{I_o}{I}$	d cm.	d_o cm.	$\frac{Nd_oL^{1.5}}{cm^{2.5}}$ sec	T lbs.	P_w
A4	0.087	94	1.600	0.0205	0.0114	1.27	0.425	19.39
		154	2.183	0.0105	0.0058	1.06	1.085	19.44
		247	3.321	0.0053	0.0029	0.85	2.941	19.43
		394	4.293	0.0037	0.0020	0.94	7.746	20.11
	0.200	94	2.121	0.0253	0.0103	1.21	0.420	19.61
		154	3.200	0.0129	0.0053	0.97	1.115	19.39
		247	4.757	0.0075	0.0031	0.91	2.863	19.36
		394	6.069	0.0056	0.0023	1.08	7.694	20.45
	0.400	94	2.983	0.0286	0.0081	0.91	0.405	19.73
		154	4.293	0.0172	0.0049	0.80	1.079	19.59
		247	5.867	0.0116	0.0033	0.97	2.787	19.66
		394	7.333	0.0089	0.0025	1.17	7.221	20.02
	0.600	94	3.211	0.0384	0.0082	0.92	0.385	19.61
		154	4.816	0.0223	0.0047	0.86	1.014	19.24
		247	6.536	0.0153	0.0033	0.97	2.640	19.47
		394	8.832	0.0108	0.0023	1.09	6.888	19.97
A3	0.087	94	1.596	0.0207	0.0115	1.50	0.365	19.47
		154	2.133	0.0109	0.0060	1.28	0.925	18.39
		247	3.052	0.0060	0.0033	1.13	2.371	18.32
		394	4.116	0.0040	0.0022	1.20	6.139	18.64
	0.198	94	2.159	0.0242	0.0099	1.29	0.360	19.65
		154	3.052	0.0137	0.0056	1.20	0.992	20.17
		247	4.317	0.0085	0.0035	1.30	2.430	19.21
		394	5.531	0.0062	0.0025	1.37	6.110	18.98
	0.399	94	2.723	0.0327	0.0093	1.21	0.345	19.65
		154	3.766	0.0204	0.0058	1.24	0.943	20.02
		247	5.364	0.0129	0.0037	1.27	2.269	18.72
		394	6.556	0.0102	0.0029	1.58	5.764	18.69
	0.600	94	3.050	0.0414	0.0088	1.05	0.330	19.66
		154	4.256	0.0261	0.0056	1.20	0.907	20.13
		247	5.719	0.0181	0.0039	1.33	2.218	19.14
		394	7.320	0.0134	0.0029	1.58	5.519	18.72
A2	0.087	94	1.439	0.0281	0.0156	1.11	0.070	18.83
		154	1.624	0.0197	0.0109	1.27	0.180	19.04
		247	2.133	0.0109	0.0060	1.12	0.485	18.90
		394	3.000	0.0062	0.0034	1.01	1.302	19.94

Table 9 (Cont'd)

Drop Diameter and Power Data for the System:
n-Butanol dispersed-Water continuous

Impeller Number	Volume Fraction BuOH	N rpm	$\frac{I_o}{I}$	d cm.	d_o cm.	$\frac{Nd_oL^{1.5}}{cm^{2.5}/sec}$	T lbs.	P_w
A2	0.198	94	1.825	0.0343	0.141	1.00	0.070	19.28
		154	2.185	0.0239	0.0098	1.14	0.180	18.47
		247	2.902	0.0149	0.0061	1.14	0.475	18.95
		394	4.023	0.0094	0.0039	1.16	1.205	18.89
	0.399	94	2.185	0.0478	0.0135	0.96	0.065	18.68
		154	2.766	0.0321	0.0091	1.06	0.175	18.74
		247	3.612	0.0217	0.0061	1.14	0.465	19.35
		394	4.917	0.0145	0.0041	1.22	1.15	18.78
	0.600	94	2.288	0.0660	0.0141	1.00	0.065	19.53
		154	2.952	0.0435	0.0093	1.08	0.170	19.03
		247	3.978	0.0285	0.0061	1.14	0.455	19.80
		394	5.382	0.0194	0.0041	1.22	1.068	18.26

Table 10

Drop Diameter and Power Data for the System:
Water dispersed-n-Butanol continuous

Impeller Number	Volume Fraction H_2O	N rpm	$\frac{I_o}{I}$	d cm.	d_o cm.	$\frac{Nd_oL^{1.5}}{cm^{2.5}/sec}$	T lbs.	P w
A4	0.100	94	1.500	0.0391	0.0208	2.33	0.365	19.95
		154	1.830	0.0236	0.0126	2.31	0.982	20.00
		247	2.440	0.0136	0.0072	2.12	2.56	20.27
		394	3.211	0.0088	0.0047	2.20	6.638	20.65
	0.200	94	1.968	0.0404	0.0165	1.84	0.370	19.74
		154	2.542	0.0254	0.0104	1.90	1.001	19.90
		247	3.211	0.0177	0.0072	2.12	2.584	19.97
		394	4.256	0.0120	0.0049	2.30	6.743	20.48
A3	0.100	94	1.441	0.0443	0.0236	3.07	0.310	19.82
		154	1.727	0.0269	0.0143	3.05	0.847	20.17
		247	2.232	0.0159	0.0085	2.91	2.131	19.73
		394	2.859	0.0105	0.0056	3.06	5.461	19.87
	0.200	94	1.849	0.0461	0.0189	2.46	--	--
		154	2.288	0.0304	0.0124	2.65	--	--
		247	2.905	0.0205	0.0084	2.88	--	--
		394	3.735	0.0143	0.0058	3.17	--	--
A2	0.100	94	1.280	0.0697	0.0372	2.64	0.060	19.34
		154	1.441	0.0442	0.0236	2.74	0.165	19.82
		247	1.679	0.0287	0.0153	2.85	0.415	19.38
		394	2.153	0.0169	0.0090	2.68	1.04	19.07
	0.200	94	1.366	0.1067	0.0436	3.09	0.060	18.88
		154	1.578	0.0675	0.0276	3.21	0.165	19.35
		247	2.103	0.0353	0.0144	2.68	0.435	19.83
		394	2.474	0.0265	0.0108	3.21	1.05	18.72

Table 11

Drop Diameter and Power Data for the System:
Methyl isobutyl ketone dispersed-Water continuous

Impeller Number	Volume Fraction MIBK	N rpm	$\frac{I_o}{I}$	d cm.	d_o cm.	$\frac{Nd_oL^{1.5}}{cm^{2.5}}$ sec	T lbs.	P_w
A4	0.087	94	1.199	0.0578	0.0320	3.58	0.375	19.30
		154	1.316	0.0364	0.0202	3.70	1.097	21.03
		247	1.549	0.0209	0.0116	3.41	3.021	22.52
		394	1.923	0.0124	0.0069	3.23	7.637	22.37
	0.202	94	1.400	0.0667	0.0274	3.06	0.369	19.45
		154	1.549	0.0485	0.0199	3.64	1.039	20.40
		247	1.882	0.0302	0.0124	3.64	2.908	22.19
		394	2.465	0.0182	0.0075	3.51	7.562	22.62
	0.307	94	1.378	0.1072	0.0360	4.02	0.335	18.05
		154	1.636	0.0638	0.0214	3.92	1.004	20.15
		247	2.083	0.0374	0.0126	3.70	2.815	21.97
		394	2.823	0.0222	0.0075	3.51	7.261	22.27
	0.414	94	1.411	0.1328	0.0369	4.13	0.332	18.30
		154	1.699	0.0782	0.0217	3.97	0.960	19.72
		247	2.188	0.0460	0.0128	3.76	2.664	21.27
		394	3.070	0.0264	0.0073	3.42	7.074	22.20
A3	0.087	94	1.346	0.0332	0.0184	2.40	0.312	19.63
		154	1.496	0.0232	0.0129	2.75	0.832	19.50
		247	1.683	0.0168	0.0093	3.18	2.320	21.13
		394	2.012	0.0114	0.0063	3.44	6.050	21.50
	0.200	94	1.606	0.0436	0.0178	2.32	0.298	19.19
		154	1.804	0.0328	0.0134	2.86	0.818	19.62
		247	2.108	0.0238	0.0097	3.32	2.264	21.11
		394	2.536	0.0172	0.0070	3.82	5.959	21.84
	0.399	94	1.651	0.0809	0.0229	2.98	0.280	18.81
		154	2.035	0.0509	0.0144	2.07	0.784	19.62
		247	2.574	0.0335	0.0095	3.25	2.123	20.66
		394	3.500	0.0211	0.0060	3.28	5.688	21.75
A2	0.087	154	1.250	0.0459	0.0254	2.95	0.205	20.55
		247	1.378	0.0304	0.0168	3.13	0.531	20.69
		394	1.563	0.0204	0.0113	3.36	1.392	21.32
	0.201	154	1.522	0.0509	0.0209	2.43	0.200	20.52
		247	1.716	0.0371	0.0152	2.83	0.508	20.27
		394	2.035	0.0256	0.0105	3.12	1.343	21.06

Table 11 (Cont'd)

Drop Diameter and Power Data for the System:
Methyl isobutyl ketone dispersed-Water continuous

Impeller Number	Volume Fraction MIBK	N rpm	$\frac{I_o}{I}$	d cm.	d_o cm.	$\frac{Nd_oL^{1.5}}{cm^{2.5}/sec}$	T lbs.	P_w
	0.401	154	1.651	0.0813	0.0230	2.67	0.195	20.88
		247	1.923	0.0573	0.0162	3.02	0.484	20.15
		394	2.465	0.0361	0.0102	3.03	1.246	20.38
B4	0.107	94	1.443	0.0305	0.0159	4.72	6.887	18.70
		151	1.743	0.0182	0.0095	4.53	17.884	18.82
		178	2.121	0.0121	0.0063	3.54	--	--
	0.214	94	1.743	0.0363	0.0144	4.28	6.684	18.56
		151	2.228	0.0220	0.0087	4.15	16.883	18.16
		178	2.588	0.0170	0.0067	3.77	--	--
	0.408	94	1.956	0.0538	0.0150	4.46	5.969	17.27
		151	2.628	0.0316	0.0088	4.20	16.114	18.07
		178	3.200	0.0234	0.0065	3.66	--	--
B3	0.107	94	1.586	0.0230	0.0120	4.42	6.387	18.06
		151	2.071	0.0126	0.0066	3.98	16.784	18.39
	0.214	94	2.047	0.0258	0.0102	3.76	6.284	18.17
		151	2.667	0.0162	0.0064	3.86	16.783	18.80
	0.408	94	2.286	0.0400	0.0112	4.13	6.069	18.29
		151	3.088	0.0246	0.0069	4.17	16.114	18.81
B2	0.107	94	1.385	0.0351	0.0183	3.67	1.407	20.10
		154	1.552	0.0244	0.0127	4.17	3.796	20.19
		247	1.957	0.0141	0.0074	3.90	9.036	18.69
		394	2.308	0.0103	0.0054	3.98	18.299	19.40
	0.214	94	1.667	0.0404	0.0160	3.21	1.323	19.32
		154	1.915	0.0295	0.0117	3.85	3.647	19.84
		247	2.222	0.0221	0.0088	4.64	8.990	19.01
		394	2.769	0.0152	0.0060	4.42	18.529	20.09
	0.408	94	1.748	0.0688	0.0192	3.85	1.192	18.14
		154	2.195	0.0430	0.0120	3.94	3.334	18.90
		247	2.727	0.0298	0.0083	4.37	8.318	18.33
		394	3.000	0.0257	0.0072	5.30	17.778	20.09
B1	0.107	247	1.549	0.0246	0.0128	2.39	0.622	20.58
		394	1.683	0.0197	0.0103	3.06	1.465	19.04

Table 11 (Cont'd)

Drop Diameter and Power Data for the System:
Methyl isobutyl ketone dispersed-Water continuous

Impeller Number	Volume Fraction MIBK	N rpm	$\frac{I_o}{I}$	d cm.	d_o cm.	$\frac{Nd_oL^{1.5}}{\frac{cm^{2.5}}{sec}}$	T lbs.	P_w
B1	0.214	247	1.768	0.0351	0.0139	2.54	0.598	20.22
		394	1.902	0.0299	0.0119	3.54	1.414	18.79
	0.311	247	1.923	0.0445	0.0150	2.80	0.606	20.92
		394	2.161	0.0354	0.0120	3.57	1.422	19.29
	0.408	247	1.882	0.0611	0.0170	3.17	0.588	20.73
		394	2.161	0.0464	0.0129	3.83	1.368	18.95

Table 12

Drop Diameter and Power Data for the System:
Water dispersed-Methyl isobutyl ketone continuous

Impeller Number	Volume Fraction H_2O	N rpm	$\frac{I_o}{I}$	d cm.	d_o cm.	$\frac{Nd_oL^{1.5}}{\frac{cm^{2.5}}{sec}}$	T lbs.	P_w
A4	0.101	94	1.326	0.0558	0.0285	3.19	0.380	17.26
		154	1.564	0.0322	0.0171	3.13	0.887	20.37
		247	1.947	0.0192	0.0102	3.00	2.455	21.92
		394	2.473	0.0123	0.0065	3.05	6.535	22.93
	0.189	94	1.551	0.0614	0.0258	2.88	0.295	17.81
		154	1.968	0.0350	0.0147	2.69	0.895	20.13
		247	2.542	0.0220	0.0092	2.70	2.538	22.19
		394	3.211	0.0153	0.0064	3.00	6.617	22.74
	0.289	94	1.710	0.0732	0.0250	2.80	0.320	18.86
		154	2.259	0.0413	0.0141	2.68	0.892	19.59
		247	2.952	0.0267	0.0091	2.67	2.551	21.78
		394	3.813	0.0185	0.0063	2.95	6.647	22.30
	0.386	94	1.830	0.0837	0.0242	2.71	0.328	18.91
		154	2.473	0.0472	0.0136	2.49	0.899	19.31
		247	3.327	0.0299	0.0086	2.53	2.611	21.79
		394	4.256	0.0213	0.0062	2.91	6.717	22.04
A3	0.100	94	1.525	0.0342	0.0182	2.37	0.245	18.27
		154	1.886	0.0203	0.0108	2.31	0.680	18.33
		247	2.205	0.0149	0.0079	2.70	1.926	21.03
		394	2.652	0.0109	0.0058	3.17	5.275	22.63
	0.201	94	1.912	0.0446	0.0182	2.37	0.255	18.76
		154	2.317	0.0275	0.0112	2.39	0.686	18.80
		247	2.731	0.0209	0.0085	2.91	1.981	21.11
		394	3.327	0.0155	0.0063	3.44	5.286	22.14
	0.401	94	2.103	0.0654	0.0185	2.41	0.273	19.17
		154	2.773	0.0407	0.0115	2.45	0.697	18.24
		247	3.327	0.0311	0.0088	3.01	2.036	20.71
		394	4.256	0.0222	0.0063	3.44	5.483	21.92
A2	0.099	154	1.441	0.0404	0.0215	2.50	0.170	20.35
		247	1.726	0.0245	0.0130	2.42	0.441	20.60
		394	2.080	0.0165	0.0088	2.62	1.147	21.05
	0.199	154	1.605	0.0592	0.0243	2.82	0.170	19.94
		247	2.011	0.0354	0.0145	2.70	0.449	20.47
		394	2.578	0.0227	0.0093	2.76	1.157	20.73

Table 12 (Cont'd)

Drop Diameter and Power Data for the System:
Water dispersed-Methyl isobutyl ketone continuous

Impeller Number	Volume Fraction H_2O	N rpm	$\frac{I_o}{I}$	d cm.	d_o cm.	$\frac{Nd_oL^{1.5}}{cm^{2.5}/sec}$	T lbs.	P_w
A2	0.398	154	1.867	0.0826	0.0233	2.71	0.180	20.16
		247	2.346	0.0532	0.0150	2.80	0.475	20.68
		394	3.327	0.0308	0.0087	2.59	1.179	20.17
B4	0.106	94	2.165	0.0157	0.0082	2.44	5.581	18.06
		154	2.921	0.0095	0.0050	2.43	15.602	18.89
		193	3.407	0.0076	0.0040	2.44	--	--
	0.203	94	2.831	0.0191	0.0078	2.32	5.669	17.92
		154	3.755	0.0127	0.0052	2.53	15.450	18.93
		182	4.219	0.0107	0.0044	2.53	--	--
	0.398	94	3.833	0.0242	0.0069	2.05	5.825	17.60
		151	4.842	0.0142	0.0040	1.91	15.559	18.21
		178	5.412	0.0156	0.0044	2.48	--	--
B3	0.106	94	2.272	0.0144	0.0075	2.76	5.381	18.13
		151	3.016	0.0091	0.0048	2.90	14.962	19.54
	0.203	94	2.921	0.0182	0.0074	2.73	5.669	18.66
		151	3.833	0.0123	0.0050	3.02	15.350	19.58
	0.398	94	3.833	0.0242	0.0069	2.54	5.825	18.32
		151	4.718	0.0184	0.0052	3.14	15.459	18.85
B2	0.106	94	1.681	0.0268	0.0140	2.81	1.116	18.99
		154	2.184	0.0154	0.0081	2.66	3.134	19.87
		247	2.836	0.0099	0.0052	2.74	7.569	18.66
		345	3.393	0.0076	0.0040	2.95	15.524	19.61
	0.203	94	2.159	0.0302	0.0123	2.47	1.149	18.67
		154	2.923	0.0182	0.0074	2.43	3.140	19.02
		247	3.826	0.0128	0.0052	2.74	7.863	18.52
		345	4.222	0.0108	0.0044	3.24	15.957	19.27
	0.398	94	2.794	0.0382	0.0108	2.17	1.151	18.29
		154	3.800	0.0245	0.0070	2.30	3.148	18.64
		247	4.524	0.0194	0.0055	2.90	8.021	18.46
		345	4.872	0.0177	0.0050	3.68	16.244	19.16

Table 12 (cont'd)

Drop Diameter and Power Data for the System:
Water dispersed-Methyl isobutyl ketone continuous

Impeller Number	Volume Fraction H_2O	N rpm	$\frac{I_o}{I}$	d cm.	d_o cm.	$\frac{Nd_oL^{1.5}}{\frac{cm^{2.5}}{sec}}$	T lbs.	P_w
B1	0.203	247	1.968	0.0378	0.0154	2.87	0.528	20.33
		394	2.905	0.0192	0.0078	2.32	1.281	19.39
	0.300	247	2.377	0.0392	0.0131	2.44	0.550	20.70
		394	3.211	0.0244	0.0082	2.44	1.285	19.01
	0.398	247	2.614	0.0444	0.0126	2.35	0.562	20.68
		394	3.389	0.0300	0.0085	2.53	1.259	18.21

Table 13

Drop Diameter and Power Data for the System:
Carbon disulfide dispersed-Water continuous
(Unbaffled Tank)

Impeller Number	Volume Fraction CS_2	N rpm	$\frac{I_o}{I}$	d cm.	d_o cm.	$\frac{Nd_oL^{1.5}}{cm^{2.5}}$ sec	T lbs.	P_w	M.I. %
A4	0.200	154	4.886	0.0345	0.0142	2.60	0.34	6.08	81
		247	6.840	0.0230	0.0095	2.79	0.87	6.05	93
		394	9.500	0.0158	0.0065	3.04	2.30	6.29	--
	0.400	154	5.516	0.0595	0.0169	3.09	0.40	6.81	92
		247	8.593	0.0354	0.0100	2.94	1.00	6.62	92
		394	13.154	0.0221	0.0063	2.95	2.42	6.28	--
A3	0.200	154	5.516	0.0297	0.0122	2.60	0.33	6.12	75
		247	7.435	0.0209	0.0086	3.05	0.94	6.79	100
		394	9.000	0.0168	0.0069	3.77	2.53	7.18	--
	0.400	154	6.107	0.0526	0.0149	3.18	0.39	6.88	86
		247	8.636	0.0351	0.0099	3.39	0.99	6.81	100
		394	14.250	0.0203	0.0058	3.17	2.69	7.27	--
A2	0.200	247	5.079	0.0329	0.0135	2.52	0.16	5.82	94
		394	7.329	0.0212	0.0087	2.58	0.47	6.71	99*
	0.400	247	5.830	0.0556	0.0158	2.94	0.17	5.88	99*
		394	8.143	0.0376	0.0107	3.18	0.52	7.07	99*

* Volume-fraction of dispersed phase larger than mean ϕ for system, hence mixing index was calculated for the opposite phase.

Table 14

Drop Diameter and Power Data for the System:
Water dispersed-Carbon disulfide continuous
(Unbaffled Data)

Impeller Number	Volume Fraction H_2O	N rpm	$\frac{I_o}{T}$	d cm.	d_o cm.	$\frac{Nd_oL^{1.5}}{cm^{2.5}/sec}$	T lbs.	P_w	M.I. %
A4	0.200	154	4.590	0.0418	0.0172	3.15	0.37	5.75	35
		247	6.885	0.0190	0.0078	2.29	0.96	5.80	75*
		394	8.136	0.0210	0.0086	4.03	2.52	5.99	--
	0.400	154	6.393	0.0556	0.0158	2.89	0.34	5.52	38
		247	8.995	0.0375	0.0107	3.14	0.92	5.81	93*
		394	11.188	0.0294	0.0083	3.89	2.43	6.04	--
A3	0.200	154	4.838	0.0391	0.0161	3.44	0.41	6.60	15
		247	7.458	0.0232	0.0095	3.25	1.07	6.72	70
		394	8.136	0.0210	0.0086	4.69	2.87	7.08	--
	0.400	154	6.885	0.0509	0.0144	3.07	0.35	5.90	18
		247	8.995	0.0375	0.0107	3.66	0.99	6.50	85
		394	11.933	0.0274	0.0078	4.26	2.67	6.86	--
A2	0.200	247	4.195	0.0469	0.0193	3.60	0.18	7.58	16
		394	5.424	0.0339	0.0139	4.13	0.53	7.57	63*
	0.400	247	5.837	0.0620	0.0176	3.28	0.18	5.95	88
		394	9.421	0.0356	0.0101	3.00	0.52	6.75	67*

*Volume-fraction of dispersed phase larger than mean ϕ for system, hence mixing index was calculated for the opposite page.

Table 15

Drop Diameter and Power Data for the System:
Methyl isobutyl ketone dispersed-Water continuous
(Unbaffled Data)

Impeller Number	Volume Fraction MIBK	N rpm	$\frac{I_o}{I}$	d cm.	d_o cm.	$\frac{Nd_oL^{1.5}}{cm^{2.5}}$ sec	T lbs.	P_w	M.I. %
A4	0.200	154	1.315	0.0839	0.0345	6.32	0.31	6.07	50
		247	1.598	0.0441	0.0181	5.32	0.83	6.33	60
		394	2.203	0.0220	0.0090	4.22	2.23	6.69	90
	0.400	154	1.523	0.1009	0.0286	5.24	0.29	5.93	35
		247	2.012	0.0521	0.0150	4.41	0.79	6.29	100
		394	2.964	0.0268	0.0076	3.56	2.05	6.42	50
A3	0.200	154	1.381	0.0692	0.0284	6.06	0.38	7.72	20
		247	1.647	0.0408	0.0167	5.72	0.94	7.45	75
		394	2.173	0.0225	0.0092	5.02	2.38	7.41	90
	0.400	154	1.552	0.0956	0.0272	5.81	0.34	7.21	37
		247	1.918	0.0575	0.0163	5.58	0.96	7.94	62
		394	2.964	0.0268	0.0076	4.15	2.30	7.47	55
A2	0.200	247	1.370	0.0714	0.0293	5.46	0.14	5.58	55
		394	1.552	0.0476	0.0196	5.83	0.42	6.58	98*
	0.400	247	1.567	0.0930	0.0264	4.92	0.14	5.82	98
		394	1.852	0.0620	0.0176	5.23	0.42	6.86	98

*Volume-fraction of dispersed phase larger than mean ϕ for system, hence mixing index was calculated for the opposite phase.

Table 16

Drop Diameter and Power Data for the System:
Water dispersed-Methyl isobutyl ketone continuous
(Unbaffled Tank)

Impeller Number	Volume Fraction H_2O	N rpm	$\frac{I_o}{I}$	d cm.	d_o cm.	$\frac{Nd_oL^{1.5}}{cm^{2.5}/sec}$	T lbs.	P_w	M.I. %
A4	0.200	154	1.621	0.0579	0.0238	4.36	0.26	5.83	46
		247	2.114	0.0323	0.0133	3.91	0.70	6.10	76
		394	2.879	0.0192	0.0079	3.70	1.80	6.17	80
	0.400	154	1.965	0.0746	0.0212	3.88	0.26	5.56	45
		247	2.651	0.0436	0.0124	3.64	0.73	6.07	75
		394	3.630	0.0274	0.0077	3.61	1.92	6.28	78
A3	0.200	154	1.687	0.0524	0.0215	4.59	0.29	6.74	55
		247	2.227	0.0293	0.0120	4.11	0.80	7.24	84
		394	2.930	0.0187	0.0077	4.20	2.10	7.48	--
	0.400	154	2.114	0.0646	0.0183	3.91	0.31	6.88	40
		247	2.694	0.0425	0.0121	4.14	0.83	7.17	90
		394	3.711	0.0265	0.0075	4.09	2.20	7.47	--
A2	0.200	247	1.687	0.0524	0.0215	4.00	0.11	5.01	84
		394	2.062	0.0339	0.0139	4.13	0.35	6.27	98
	0.400	247	2.114	0.0646	0.0183	3.41	0.12	5.22	83
		394	2.530	0.0470	0.0133	3.95	0.37	6.32	100

Table 17

Drop Diameters and Power Data for the System:
Carbon tetrachloride-Water
(Unbaffled Tank)

Impeller Number	Volume Fraction CCl_4	N rpm	$\frac{I_o}{I}$	d cm.	d_o cm.	$\frac{Nd_oL^{1.5}}{cm^{2.5}}$ sec	T lbs.	P_w	M.I. %
A4	0.200	247	3.000	0.0327	0.0134	3.93	0.91	5.95	94
		394	6.107	0.0128	0.0053	2.48	2.39	6.15	--
	0.400	247	4.622	0.0361	0.0103	3.03	1.05	6.21	98*
		394	7.773	0.0193	0.0055	2.58	2.72	6.33	--
	Volume Fraction H_2O								
A4	0.200	247	2.949	0.0475	0.0195	5.73	1.16	5.75	79*
		394	6.214	0.0149	0.0061	2.86	3.12	6.09	--
	0.400	247	4.703	0.0500	0.0142	4.17	1.07	5.77	90*
		394	7.565	0.0282	0.0080	3.75	2.86	6.07	--

*Volume-fraction of dispersed phase larger than mean ϕ for system, hence mixing index was calculated for the opposite phase.

Table 18

Average values of b, the slope of log d versus $(\phi)^{0.5}$
(Dispersed phase listed first)

Baffled data:

	System	Impeller Size	b Slope
1.	Butanol-Water	A4	1.90
2.	Water-Butanol	A4	1.65
3.	Butanol-Water	A2	1.97
4.	Water-Butanol	A2	2.42
5.	Butanol-Water	A3	2.03
6.	Water-Butanol	A3	1.60
7.	Methyl isobutyl ketone-Water	A2	1.83
8.	Water-Methyl isobutyl ketone	A2	2.09
9.	Methyl isobutyl ketone-Water	A3	2.25
10.	Water-Methyl isobutyl ketone	A3	1.80
11.	Methyl isobutyl ketone-Water	A4	2.27
12.	Water-Methyl isobutyl ketone	A4	1.70
13.	Methyl isobutyl ketone-Water	B1	2.75
14.	Water-Methyl isobutyl ketone	B1	1.95
15.	Methyl isobutyl ketone-Water	B2	2.30
16.	Water-Methyl isobutyl ketone	B2	1.97
17.	Methyl isobutyl ketone-Water	B3	1.87
18.	Water-Methyl isobutyl ketone	B3	1.95
19.	Methyl isobutyl ketone-Water	B4	1.90
20.	Water-Methyl isobutyl ketone	B4	1.78
21.	Carbon tetrachloride-Water	A4	1.78
22.	Water-Carbon tetrachloride	A4	2.45
23.	Carbon disulfide-Water	A2	2.15
24.	Water-Carbon disulfide	A2	1.98
25.	Carbon disulfide-Water	A3	1.95
26.	Water-Carbon disulfide	A3	2.08
27.	Carbon disulfide-Water	A4	1.89
28.	Water-Carbon disulfide	A4	2.71
29.	Iso-octane-Water	A4	1.70
30.	Water-Iso-octane	A4	1.82

Average value of slope, b, for all systems = 2.02 ± 0.40

Table 18 (Cont'd)

Average values of b, the slope of log d versus $(\phi)^{0.5}$
(Dispersed phase listed first)

Unbaffled data:

	System	Impeller Size	b Slope
1.	Methyl isobutyl ketone-Water	A2	1.42
2.	Water-Methyl isobutyl ketone	A2	1.43
3.	Methyl isobutyl ketone-Water	A3	1.51
4.	Water-Methyl isobutyl ketone	A3	1.65
5.	Methyl isobutyl ketone-Water	A4	1.01
6.	Water-Methyl isobutyl ketone	A4	1.58
7.	Carbon tetrachloride-Water	A4	1.36
8.	Water-Carbon tetrachloride	A4	1.86
9.	Carbon disulfide-Water	A2	2.94
10.	Water-Carbon disulfide	A2	0.89
11.	Carbon disulfide-Water	A3	2.30
12.	Water-Carbon disulfide	A3	1.62
13.	Carbon disulfide-Water	A4	2.36
14.	Water-Carbon disulfide	A4	2.33

Average value of slope, b, for all systems = 1.80 ± 0.50.

Table 19

Average values of $Nd_oL^{1.5}$

Baffled Tank	$(Nd_oL^{1.5})_{avg.}$ $\frac{cm^{2.5}}{sec}$
Carbon tetrachloride-Water	1.62
Water-Carbon tetrachloride	2.17
Carbon disulfide-Water	1.95
Water-Carbon disulfide	2.48
Iso-octane-Water	2.09
Water-Iso-octane	5.16
Butanol-Water	1.14
Water-Butanol	2.65
Methyl isobutyl ketone-Water (small tank)	3.28
Water-Methyl isobutyl ketone (small tank)	2.76
Methyl isobutyl ketone-Water (large tank)	3.88
Water-Methyl isobutyl ketone (large tank)	2.61
Unbaffled Tank	
Carbon tetrachloride-Water	3.01
Water-Carbon tetrachloride	4.13
Carbon disulfide-Water	2.99
Water-Carbon disulfide	3.49
Methyl isobutyl ketone-Water	5.18
Water-Methyl isobutyl ketone	3.98